The 2 ^1A_g state of *trans,trans*-1,3,5,7-octatetraene in free jet expansions

Hrvoje Petek,[a] Andrew J. Bell,[b] Young S. Choi,[c] and Keitaro Yoshihara
Institute for Molecular Science, Myodaiji, Okazaki 444, Japan

Brett A. Tounge and Ronald L. Christensen
Department of Chemistry, Bowdoin College, Brunswick, Maine 04011

(Received 6 May 1992; accepted 20 November 1992)

One- and two-photon fluorescence excitation and emission spectra of the $S_1 \leftrightarrow S_0$ transition of *trans,trans*-1,3,5,7-octatetraene have been measured for the first time in free jet expansions. The one-photon excitation spectrum is the same, with the exception of significant differences in the intensities of a few lines, as the two-color, resonance-enhanced, two-photon ionization spectrum, previously assigned to the 2 $^1A' \leftarrow 1\ ^1A'$ transition of *cis,trans*-1,3,5,7-octatetraene. However, comparison of the one- and two-photon fluorescence excitation spectra shows clearly that the carrier of the spectrum has inversion symmetry, as expected for *trans,trans*-1,3,5,7-octatetraene. The one-photon spectrum is built on b_u Herzberg–Teller promoting modes, which are origins of progressions in a_g modes, while the two-photon spectrum is due to a single progression in a_g modes starting from the 2 $^1A_g \leftarrow 1\ ^1A_g$ electronic origin. The appearance of out-of-plane vibrations, possibly including torsions of the polyene framework, suggests large differences in force constants and perhaps in the geometries of the 2 ^1A_g and 1 ^1A_g potential surfaces. For 2 ^1A_g vibronic levels with energies $< 1000\ cm^{-1}$, the fluorescence lifetimes vary between 170 and 450 ns due to the dependence of radiative and nonradiative decay rates on the vibronic state. An abrupt increase in the nonradiative decay rates at $\sim 2100\ cm^{-1}$ excess energy is tentatively ascribed to *trans*→*cis* isomerization. This work demonstrates that the one- and two-photon cross sections of the 2 $^1A_g \leftarrow 1\ ^1A_g$ transitions of *all-trans* linear polyenes are sufficiently large to allow the study of 2 ^1A_g states under isolated, unperturbed conditions.

I. INTRODUCTION

The electronic spectroscopy of *trans,trans*-1,3,5,7-octatetraene, a prototypical linear polyene, has provided a great deal of information on the electronic structure and dynamics of simple conjugated molecules.[1,2] Tetraenes are the shortest polyenes with significant fluorescence quantum yields in both condensed and gas phases. They also are the longest polyenes for which reliable *ab initio* calculations are available.[1–3] Detailed studies of these systems provide the basis for understanding the excited states of longer polyenes, which play important roles in biological processes such as vision and bacterial and plant photosynthesis.[4,5] Long polyenes also are being investigated for their applications as materials with useful nonlinear optical and electronic properties.[6,7] To provide experimental benchmarks for a theoretical understanding of polyene excited states, it is desirable to study the properties of *trans,trans*-1,3,5,7-octatetraene under isolated conditions. Measurements of the photophysical and photochemical properties of octatetraene under low temperature, isolated conditions also provide a point of reference for investigating the effects of environment and substitution on the structure and dynamics of polyenes.

The optical spectroscopy of linear polyenes is governed by two low-lying electronic states—the ionic 1 ^1B_u (S_2) state and the covalent 2 ^1A_g (S_1) state (C_{2h} symmetry labels often are applied to linear polyenes even when the molecules do not have inversion symmetry).[1,2] Hudson and Kohler were the first to demonstrate that the lowest excited state of 1,8-diphenyl-1,3,5,7-octatetraene is not due to the strongly allowed, 1 $^1B_u \leftarrow 1\ ^1A_g$, lowest unoccupied molecular orbital←highest occupied molecular orbital (LUMO←HOMO) transition predicted by simple molecular orbital theories.[8] Their work proved that in most linear polyenes, the lowest energy excited state is 2 ^1A_g, for which the transition moment is too weak to observe 2 $^1A_g \leftarrow 1\ ^1A_g$ spectra by conventional absorption techniques.[8] Theoretical calculations by Shulten, Ohmine, and Karplus[9,10] showed that the mixing of singly and doubly excited A_g configurations results in a lowering of the 2 ^1A_g energy below that of the 1 ^1B_u state.

Even though the cross section for absorption to the 2 ^1A_g state is small, it can be populated efficiently from the 1 ^1B_u state by internal conversion on femtosecond time scales.[11] Subsequent chemistry occurs in the longer lived 2 ^1A_g state, which may decay by *cis–trans* isomerization.[12] The rates of internal conversion and isomerization are determined by couplings among the S_0, S_1, and S_2 states and surface crossings which occur at large torsional angles.[13–15] The interactions between the ground state and lowest excited singlet states have a number of manifestations in high resolution absorption and emission spectra. The broad ($\geqslant 14\ cm^{-1}$) Lorentzian linewidths observed in $S_2 \leftarrow S_0$

[a]Present address: Advanced Research Laboratory, Hitachi Ltd., Hatoyama, Saitama 350-03, Japan.
[b]Present address: Department of Chemistry, The University of Southampton, Highfield, Southampton S09 5NH United Kingdom.
[c]Present address: Department of Chemistry, Inha University, Incheon 452-751, South Korea.

 0021-9606/93/053777-18$06.00

spectra of tetraenes[16–19] most likely are due to conical intersections between the S_2 and S_1 states and are consistent with $S_2 \rightarrow S_1$ internal conversion on subpicosecond time scales.[20,21] It has been demonstrated in condensed phase samples that the forbidden $2\,^1A_g \leftarrow 1\,^1A_g$ transition has sufficient oscillator strength to be observed in fluorescence excitation spectra due to strong Herzberg–Teller coupling[22] between the $1\,^1B_u$ and $2\,^1A_g$ states, which is induced by b_u vibrations. As a result, the one-photon $2\,^1A_g \leftarrow 1\,^1A_g$ spectra of linear polyenes with inversion symmetry consist of progressions in Franck–Condon active a_g modes beginning at several $1 \leftarrow 0$ origins due to b_u promoting modes.[23–25]

Vibrational motions which change the energy gaps between polyene low-lying electronic states promote radiationless decay of the S_2 and S_1 states.[12,13,26] For example, Zerbetto and Zgierski have shown that a_g C=C stretching as well as b_g out-of-plane distortions enhance nonradiative decay in butadiene.[13] Vibronic coupling between S_1 and S_0 is manifested by anomalously high CC stretching frequencies in the S_1 state and correspondingly low CC stretching frequencies in the S_0 state.[21,23,27] Inversion of CC bonds orders between the S_0 and S_1 states results in a significant reduction in the activation energies for *cis–trans* isomerization about C=C bonds in the S_1 state.[1,2,14,15] The displacement of the S_1 and S_0 potential surfaces in the CC stretching coordinates gives these modes large Franck–Condon factors in absorption and emission. Large Franck–Condon factors and the high vibrational frequencies make C=C stretches good accepting modes for internal conversion.[12,13,26,27]

In free jet expansions, the $2\,^1A_g$ states of trienes and tetraenes exhibit rapid nonradiative decay processes with activation energies of <200 and ~ 2000 cm^{-1}, respectively.[20,21,28] These decays may be due to *cis–trans* isomerization, though at present, there is no proof of this conjecture. Since many of the photobiological functions of polyenes involve excited state, *cis–trans* isomerization, it is essential to understand the details of this process in model systems under vibronically resolved, collision-free conditions.

Most of the information on the low-lying electronic states of linear polyenes has been obtained in mixed crystals at low temperatures.[23,25,29] These studies have provided an understanding of the structure and dynamics of polyenes and how these properties are influenced by solvent environment.[30–32] Also, because of its large transition moment, it has been possible to measure the one-photon absorption[16] and laser induced fluorescence[17] spectra of the $S_2 \leftrightarrow S_0$ transition of octatetraene in supersonic molecular beams. However, the $S_1 \leftrightarrow S_0$ transition had not been studied in the gas phase, in large part because of reports of vanishingly small S_1 state fluorescence quantum yields under isolated conditions.[1,2,33]

Two recent developments have provided new tools for studying polyenes in molecular beams. Kohler and coworkers applied the resonance enhanced multiphoton ionization (REMPI) technique to detect $S_1 \leftarrow S_0$ spectra of *cis*-hexatriene[33] and several *cis* isomers of alkyl substituted trienes.[34] The observation of only minor *cis*-isomer impurities was attributed to extremely small oscillator strengths for the symmetry forbidden $2\,^1A_g \leftarrow 1\,^1A_g$ transitions of *trans* isomers.[33,34] The REMPI technique was later extended to measure the $S_1 \leftarrow S_0$ spectrum of a mixture of octatetraene isomers using two-color, resonance enhanced, two-photon ionization (2C-RE2PI).[35] This spectrum was assigned to the *cis,trans* isomer because only *cis* trienes had observable REMPI spectra.[33] In parallel with the REMPI experiments on trienes, Bouwman *et al.* discovered $S_2 \rightarrow S_0$ and $S_1 \rightarrow S_0$ emissions of tetraenes and pentaenes both as room temperature vapors and in supersonic jets.[18] Subsequently, the fluorescence excitation and emission spectra of the $S_2 \leftrightarrow S_0$ and $S_1 \leftrightarrow S_0$ transitions of methyl substituted tetraenes, *all-trans*-decatetraene, and *all-trans*-nonatetraene were measured in He expansions.[19–21] Fluorescence techniques also were applied to the trienes where nonradiative decay at very low excess energies could be deduced from fluorescence lifetimes and relative fluorescence quantum yields.[28]

We report here the one- and two-photon $S_1 \leftarrow S_0$ fluorescence excitation spectra and $S_1 \rightarrow S_0$ emission spectra of $>99\%$ pure *trans,trans*-octatetraene in He supersonic jets. The one-photon $S_1 \leftarrow S_0$ spectrum is essentially the same as that observed in the 2C-RE2PI study,[35] but here is assigned to the *trans,trans*-octatetraene isomer. This is based on the comparison between the one- and two-photon spectra, which shows that the gerade and ungerade inversion symmetry labels are strictly valid as expected for *trans,trans*-octatetraene. This assignment is further substantiated by careful examination of the one-photon, vibronically allowed $S_1 \leftrightarrow S_0$ spectra, including the analysis of hot-band structure and comparison of vibrational frequencies with those observed in corresponding spectra of low temperature mixed crystals. These findings resolve the important question of whether the one- and two-photon cross sections of the $2\,^1A_g \leftarrow 1\,^1A_g$ transitions of *all-trans*-linear polyenes are sufficiently large to be detected under conditions where the center of molecular symmetry is rigorously maintained. Analyses of the $2\,^1A_g$–$1\,^1A_g$ spectra and the dependence of fluorescence lifetimes on vibronic energy level also provide new information on the structure and couplings between polyene electronic states and nonradiative decay processes (possibly including *trans* $\rightarrow$ *cis* isomerization) in the $2\,^1A_g$ state.

II. EXPERIMENT

Octatetraene samples of high purity were prepared as follows: 2,4-hexadienal was reacted with vinylmagnesium bromide following the procedures described by D'Amico *et al.*[36] to produce 1,4,6-octatrien-3-ol. Dehydration of 1,4,6-octatrien-3-ol at 80 °C using *p*-toluene sulfonate catalyst following the procedure of Yoshida *et al.*[37] yielded $>99\%$ isomerically pure *trans,trans*-1,3,5,7-octatetraene. Such high purity can be achieved because the dehydration procedure requires much lower temperature than in conventional synthesis.[36] Crystalline samples were kept at -80 °C before use in the experiments.

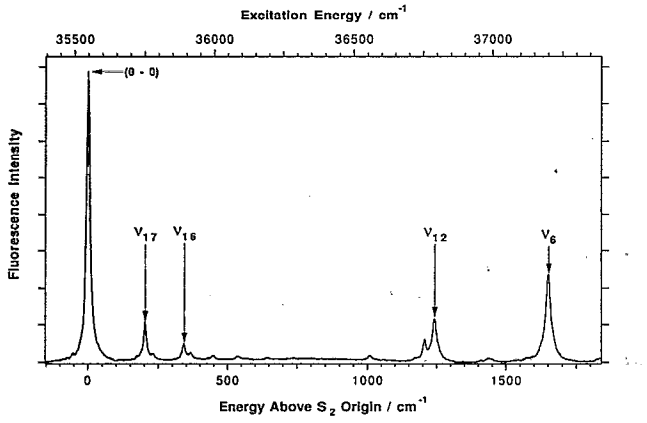

FIG. 1. The $S_2 \leftarrow S_0$ fluorescence excitation spectrum of *trans,trans*-1,3,5,7-octatetraene in a He free jet expansion. The spectrum is presented to show the high isomeric purity of the *trans,trans*-octatetraene sample. Assignments of some of the stronger lines are indicated.

Since the $S_2 \leftarrow S_0$ absorption spectra of *trans,trans*-octatetraene and *cis,trans*-1,3,5,7-octatetraene are symmetry allowed, the isomeric composition of the sample could be checked *in situ* by measuring the $S_2 \leftarrow S_0$ fluorescence excitation spectrum of our samples. Figure 1 shows the $S_2 \leftarrow S_0$ fluorescence excitation spectrum of the region where both isomers are expected to absorb. The spectrum is assigned exclusively to *trans,trans*-octatetraene based on the previous $S_2 \leftarrow S_0$ absorption,[16] fluorescence excitation,[17] and 2C-RE2PI spectra.[35] There is no feature corresponding to the *cis,trans*-1,3,5,7-octatetraene, whose $S_2 \leftarrow S_0$ origin was reported by Buma *et al.* at 73 cm^{-1} below the *trans,trans* origin.[35] Although the relative strengths of $S_2 \leftarrow S_0$ transitions and fluorescence quantum yields of the two isomers are not known, the observation of the $S_2 \leftarrow S_0$ origins, which have comparable linewidths and about the same relative intensities as expected from the isomeric composition of the sample in the 2C-RE2PI spectra,[35] suggests that the fluorescence technique has nearly the same sensitivity for both isomers. Impurity lines with intensities of less than 1% of the main lines could be seen in the $S_1 \leftarrow S_0$ spectra. The relative intensities of these lines varied from sample to sample, and decreased with respect to the main lines during the course of an experiment, as expected for impurities with higher vapor pressures than the *trans,trans* isomer. On the basis of the absence of *cis,trans*-1,3,5,7-octatetraene features in the $S_2 \leftarrow S_0$ fluorescence excitation spectrum, we conclude that our octatetraene sample contains $<1\%$ of the *cis,trans* isomer.

The experimental apparatus for measuring fluorescence excitation spectra, fluorescence spectra, and fluorescence lifetimes was essentially the same as previously used for experiments on methyl substituted trienes and tetraenes.[19,28] The octatetraene concentration was controlled by fixing the sample reservoir temperature at 35 °C for fluorescence excitation spectra and lifetime studies, and at 35–50 °C for emission spectra. Hot bands from population of low frequency b_u states at low He stagnation pressures (150–480 Torr) were useful for estimating the energy of the $S_1 \leftarrow S_0$ origin from one-photon excitation spectra. Stagnation pressures of ~500–800 Torr gave spectra of vibrationally and rotationally cold molecules. Under these experimental conditions, the octatetraene sample was sufficiently stable to make useful measurements for >12 h. Some polymerization may have occurred during the course of the experiments. However, the polymerization products did not interfere with the spectroscopic measurements.

The one-photon $S_1 \leftarrow S_0$ spectrum was recorded using several overlapping scans from 347 to 300 nm using a Lambda-Physik EMG104/3002 excimer pumped dye laser with PTP and frequency-doubled outputs of sulforhodamine 101 and rhodamine B dyes. The excitation energy was $<500\ \mu J$ and the laser beam collimated to ~2 mm diam to avoid saturation of transitions. A composite spectrum was assembled by matching the intensities of individual scans in the overlapping spectral regions. Laser scan intervals of 0.0025 nm between 347 and 314.5 nm and 0.005 nm between 314.5 and 300 nm gave sufficient resolution to accurately measure line positions and intensities. The $S_2 \leftarrow S_0$ spectrum was recorded using the second harmonic of the coumarin 153 dye. Since the vibronic lines are much broader than for the $S_1 \leftarrow S_0$ transition, the laser scan interval was increased to 0.025 nm. The excitation energy had to be reduced to $<1\ \mu J$ to prevent saturation of this strongly allowed transition. The optogalvanic spectrum of a Ne hollow-cathode lamp provided a wavelength calibration for the spectra. Excellent signal-to-noise ratios could be obtained by averaging ten laser shots at a 10 Hz repetition rate for each scan interval.

The two-photon $S_1 \leftarrow S_0$ spectrum was recorded from 691 to 674.5 nm using a Lambda-Physik LPX100/LPD3000 excimer pumped dye laser operating with pyridine 1 dye. The dye laser output energy was 10–20 mJ in this scan region. The beam was focused by a 600 mm f.l. lens to ~100 mm in front of the molecular beam. This gave the largest signal of ~50 detected photons/pulse at the origin. The beam diameter in the interaction region was estimated to be <0.3 mm from its burn pattern. The signal was separated from scattered light with a Schott BG28 filter. The spectra were not normalized for the excitation laser intensity. The laser scan step size was 0.0025 nm.

Emission spectra were measured for selected vibronic levels with low excess vibrational energy. A 250 mm focal length spectrograph, equipped with a 600 lines/mm grating blazed at 300 nm, dispersed the emission, and an intensified multichannel diode array detector with a 25 μm spacing between elements (EG&G PAR 1420) recorded the spectrum with a resolution of ~10 cm^{-1}/point. The input slit width was 100 μm. Spectra were recorded by exciting the sample at a 15 Hz laser repetition rate and integrating the signal for 3–5 min. Emission from a low pressure mercury lamp provided calibration spectra. Peak positions were determined by fitting Gaussian profiles to the observed lines.

Fluorescence lifetimes were recorded with a LeCroy 9400 digital oscilloscope by summing 200–500 decay traces for one-photon excitation and 2000–5000 traces for two-photon excitation. The time resolution of the decay mea-

surements was limited both by the 175 MHz bandwidth of the oscilloscope and the 15 ns pulse width of the excitation laser. Fitting the fluorescence decay profiles to single exponential decays gave the reported lifetimes. For higher energy vibronic states, it was necessary to convolute the laser pulse shape to extract accurate lifetimes. Since the measured lifetimes are significantly different from those reported in Ref. 35, the digital oscilloscope time base was calibrated against two reference sources. The accuracy was found to be better than 1% on the time scales used to measure the lifetimes. Systematic errors in the lifetime measurements are estimated to be $<5\%$ for intense lines with $<1000\ \text{cm}^{-1}$ excess energy based on comparison of repeated measurements on same vibronic states under different experimental conditions.

III. RESULTS AND DISCUSSION

A. Carrier of spectra

One of the most important results of this study is to establish that the carrier of the spectra is *trans,trans*-1,3,5,7-octatetraene, rather than *cis,trans*-octatetraene.[35] The *trans,trans*- and *cis,cis*-octatetraene isomers can be distinguished from the *cis,trans*-octatetraene by the absence of inversion symmetry in the *cis,trans* isomer. The $2\,^1A' \leftarrow 1\,^1A'$ transition of *cis,trans*-octatetraene is electric-dipole allowed for both one- and two-photon excitations. In both cases, optical transitions only couple bands of the same symmetry, and the one- and two-photon spectra should coincide. By contrast, the one-photon $S_1 \leftarrow S_0$ spectra of *trans,trans*- and *cis,cis*-octatetraene are electric-dipole forbidden and the two-photon spectra are allowed. The transition moments of $2\,^1A_g \leftrightarrow 1\,^1A_g$ spectra are derived from vibronic coupling between the ^1A_g and ^1B_u states via b_u vibrations. Therefore, the one-photon $2\,^1A_g \leftrightarrow 1\,^1A_g$ spectra are restricted to transitions where the direct product of the initial and final vibronic states has b_u symmetry. Absorption spectra of vibrationally cold molecules thus should consist of $\Delta v = +1$ transitions in b_u promoting modes with the intensities determined by the strength of S_2–S_1 coupling induced by each mode. Franck–Condon active a_g modes can only appear in combination with b_u promoting modes. Weaker bands may involve $\Delta v = +1$ transitions of several antisymmetric modes with an overall change corresponding to b_u symmetry. Emission spectra are expected to show similar vibronic behavior.

Comparison of the one- and two-photon spectra near the $S_1 \leftarrow S_0$ electronic origin (Fig. 2) provides both the

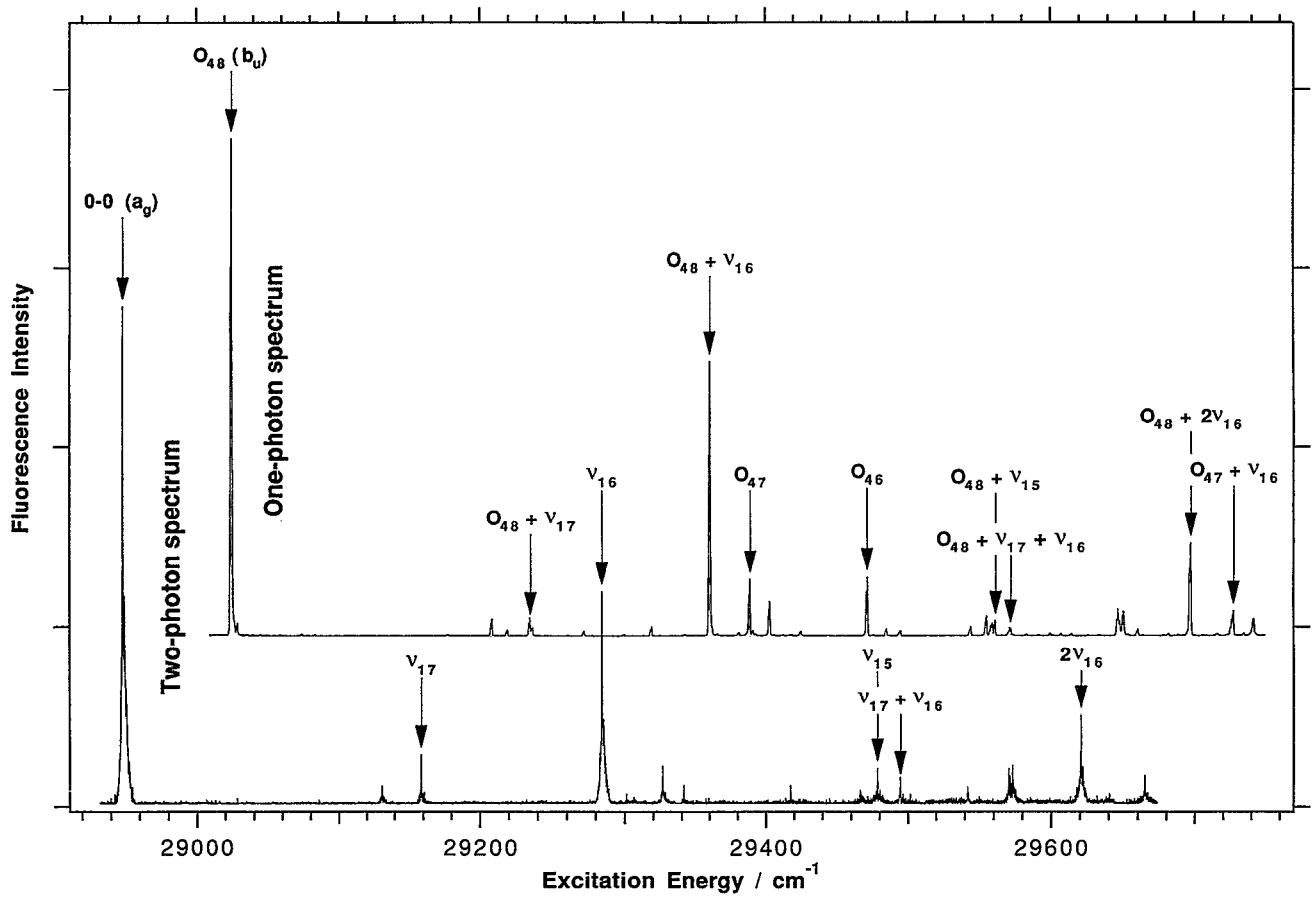

FIG. 2. A comparison of the one- and two-photon fluorescence excitation spectra of the $2\,^1A_g \leftarrow 1\,^1A_g$ transition of *trans,trans*-1,3,5,7-octatetraene. The assignments show that the two-photon spectrum is a progression in Franck–Condon active a_g vibrations and the one-photon spectrum is due to b_u Herzberg–Teller promoting modes (O_{48}, O_{47}, and O_{46}), which are origins for a_g Franck–Condon progressions.

TABLE I. Assignments, vibrational frequencies, intensities, and lifetimes of stronger lines in the one- and two-photon $S_1 \leftarrow S_0$ spectra of *trans,trans*-octatetraene. The two-photon frequencies are measured relative to the $0 \leftarrow 0$ origin at 28 948.7 cm^{-1} and the one-photon frequencies are measured relative to the $1 \leftarrow 0$ origin O_{48} at 29 024.9 cm^{-1}. For combination bands and overtones, Δ is the difference between the observed frequencies and the sum of the fundamental frequencies.

Assignment[a]	Frequency (cm^{-1})	Δ	Intensity	Lifetime (ns)
Two photon				
0–0	0		[b]	446
	182.4			442
ν_{17}	210.1			410
	212.4			
	247.0			
	294.5			
ν_{16}	336.0			434
	378.1			312
	469.1			
	518.4			221
ν_{15}	530.2			401
$\nu_{16}+\nu_{17}$	546.2	0.1		365
	593.7			262
	622.2			157
	623.2			163
	624.7			163
$2\nu_{16}$	672.4	0.4		395
	716.7			274
One photon				
ν_{48} (1–0,b_u)	(0)		(100.0)	341
Cis,trans[c]	33.4		0.2	
Cis,trans	48.8		0.3	281
$3\nu_{48}$	153.1		0.3	
	183.3		3.2	326
	193.9		1.2	377
$\nu_{48}+\nu_{17}$	209.7		3.5	337
	211.6		1.6	378
Cis,trans	235.9		0.1	
	246.8		0.8	315
	293.7		1.8	314
$\nu_{48}+\nu_{16}$	335.7		55.2	337
ν_{47} (b_u)	363.7		11.0	322
	377.8		6.6	297
$\nu_{48}+2\nu_{17}$	419.2	−0.2	0.1	
ν_{46} (b_u)	446.7		11.6	318
	459.7		1.3	293
	469.9		0.9	305
	519.2		1.7	323
$\nu_{48}+\nu_{15}$	529.9		3.7	314
	532.7		1.8	373
	534.3		2.5	231
	536.2		2.9	203
$\nu_{48}+\nu_{16}+\nu_{17}$	546.0	0.6	0.8	
	547.5		1.2	352
$\nu_{47}+\nu_{17}$	574.6	1.2	0.7	
	621.9		5.1	170
	622.6		2.8	199
	625.2		4.7	219
	635.1		1.2	267
$\nu_{46}+\nu_{17}$	656.8	0.4	0.4	
$\nu_{48}+2\nu_{16}$	672.2	0.8	18.5	331
$\nu_{47}+\nu_{16}$	700.8	1.4	3.1	277
	702.2		4.8	303
	716.7		3.3	289
	732.8		1.7	244
$\nu_{46}+\nu_{16}$	780.4	−2.0	9.8	322
	794.4		1.3	240
	805.0		4.3	316
	817.5		1.8	243
	824.4		1.5	303
$\nu_{48}+\nu_{15}+\nu_{16}$	865.8	0.2	2.5	284
	868.8		1.7	

TABLE I. (*Continued.*)

Assignment[a]	Frequency (cm^{-1})	Δ	Intensity	Lifetime (ns)
	870.5		8.7	231
	873.3	1.4	6.3	253
ν_{45} (b_u)	875.4		5.1	240
$\nu_{48}+2\nu_{16}+\nu_{17}$	883.3	2.2	0.7	
$\nu_{47}+\nu_{17}$	894.3	0.7	0.2	
	922.5		1.5	242
	957.8		2.2	227
$\nu_{48}+\nu_{14}$	964.8		4.3	242
ν_{44} (b_u)	967.8		3.2	220
	970.2		5.2	258
$\nu_{46}+\nu_{15}$	978.6	2.0	1.0	
	1003.7		1.1	266
$\nu_{48}+3\nu_{16}$	1009.1	2.0	3.2	286
	1061.0		1.1	248
$\nu_{48}+\nu_{13}$	1080.0		8.9	212
$\nu_{45}+\nu_{17}$	1084.4	−0.5	0.4	
$\nu_{45}+\nu_{16}$	1210.8	−0.3	4.2	196
$\nu_{48}+\nu_{12}$	1225.2		45.4	235
$\nu_{48}+\nu_{11}$	1275.5		8.4	203
$(\nu_{48}+\nu_{10})$[d]	1279.6		4.9	201
$(\nu_{48}+\nu_9)$	1283.8		2.5	197
$\nu_{48}+\nu_{13}+\nu_{17}$	1289.1	0.6		
$\nu_{48}+\nu_{16}+\nu_{14}$	1300.0			
	1302.3		2.7	194
$\nu_{44}+\nu_{16}$	1303.5	0.0	2.2	
$\nu_{48}+4\nu_{16}$	1343.3	0.5	0.1	
$\nu_{48}+\nu_{13}+\nu_{16}$	1415.7	0.0	5.7	179
$\nu_{48}+\nu_{12}+\nu_{17}$	1436.5	1.6	1.0	
$\nu_{47}+\nu_{13}$	1444.2	0.5	1.6	
ν_{39} (b_u)	1477.8		10.4	173
	1490.1		3.2	174
	1498.7		3.7	174
$\nu_{48}+\nu_7$	1508.7		8.8	169
ν_{38} (b_u)	1515.0		18.7	171
$\nu_{46}+\nu_{13}$	1526.9	0.3	0.5	
	1532.3		3.3	169
$\nu_{45}+2\nu_{16}$	1545.3	0.6	2.2	
$\nu_{48}+\nu_{12}+\nu_{16}$	1560.9	0.0	23.8	166
$\nu_{47}+\nu_{12}$	1588.3	−0.6	5.3	164
$\nu_{48}+\nu_{11}+\nu_{16}$	1610.8	−0.4	4.6	
$(\nu_{48}+\nu_{10}+\nu_{16})$	1615.4	0.1	2.1	
$(\nu_{48}+\nu_9+\nu_{16})$	1619.4	−0.1	2.0	
$\nu_{47}+\nu_{11}$	1638.4	−0.8	2.5	
$\nu_{46}+\nu_{12}$	1670.9	−1.0	4.1	157
$\nu_{48}+\nu_{13}+2\nu_{16}$	1752.0	0.6	1.4	
$\nu_{48}+\nu_{15}+\nu_{12}$	1755.3	0.2	1.6	
$\nu_{48}+2\nu_{13}+2\nu_{16}$	1758.9	0.4	1.8	
	1787.5		8.2	148
$\nu_{48}+\nu_6$	1797.9		92.0	145
$\nu_{39}+\nu_{16}$	1812.4	−1.1	5.3	149
$\nu_{48}+\nu_7+\nu_{16}$	1843.3	−1.1	5.5	136
$\nu_{38}+\nu_{16}$	1849.3	−1.1	13.1	137
$\nu_{47}+\nu_7$	1870.2	−1.4	2.6	140
$\nu_{48}+\nu_{12}+2\nu_{16}$	1897.2	−2.2	7.0	137
$\nu_{47}+\nu_{12}+\nu_{16}$	1926.7	2.1	2.5	120
$\nu_{48}+2\nu_{16}+\nu_{11}$	1947.3	0.4	1.1	
$\nu_{46}+\nu_7$	1954.2	1.2	1.5	
	1981.4	0.2	2.3	112
$\nu_{48}+\nu_{17}+\nu_6$,	2007.9	0.3	3.6	110
and/or $\nu_{46}+\nu_{12}+\nu_{16}$,		0.3		
and/or $\nu_{39}+\nu_{15}$		0.2		
	2029.6		2.4	109
$\nu_{48}+\nu_{14}+\nu_{13}$,	2044.1	−0.7	0.8	
and/or $\nu_{38}+\nu_{15}$		−0.8		
	2046.4		1.0	100
$\nu_{48}+\nu_{16}+\nu_{15}+\nu_{12}$	2090.4		1.0	

TABLE I. (*Continued.*)

Assignment[a]	Frequency (cm^{-1})	Δ	Intensity	Lifetime (ns)
$\nu_{45}+\nu_{12}$	2097.7	−2.9	1.1	58
	2123.0		2.1	59
$\nu_{48}+\nu_6+\nu_{16}$	2132.7		17.1	60
$\nu_{39}+2\nu_{16}$, and/or	2148.3	−0.9	1.9	49
$\nu_{45}+\nu_{11}$		−2.6		
$\nu_{48}+2\nu_{13}$,	2158.2	−1.6	3.1	44
and/or $\nu_{47}+\nu_6$		−3.2		
	2174.9		1.6	44
$\nu_{38}+2\nu_{16}$	2184.2	−2.2	0.9	44
$\nu_{44}+\nu_{12}$	2193.7	0.7	0.6	
	2216.3		1.1	78
	2221.0		0.9	58
$\nu_{48}+\nu_{12}+3\nu_{16}$	2233.6	1.3	0.4	
$\nu_{46}+\nu_6$	2241.7	−2.9	1.7	28
$\nu_{48}+\nu_{12}+\nu_{13}$	2302.8	−2.4	0.5	21
$\nu_{15}+\nu_6$	2327.8	0.0	0.3	
	2337.2		0.7	19
	2430.3		1.3	13
$\nu_{48}+2\nu_{12}$	2448.9	−1.5	2.2	12
$\nu_{48}+\nu_6+2\nu_{16}$	2467.2	−2.1	1.7	12
$\nu_{47}+\nu_6+\nu_{16}$, and/or	2494.3	−3.0	0.6	
$\nu_{48}+2\nu_{13}+\nu_{16}$		−1.4		
$\nu_{48}+\nu_{11}+\nu_{12}$	2498.3	−2.4	0.5	
$(\nu_{48}+\nu_{12}+\nu_{10})$	2503.3	−1.5	0.3	
$\nu_{46}+\nu_6+\nu_{16}$	2573.8	−6.5	0.5	
$\nu_{38}+\nu_{13}$	2591.3	−3.7	0.2	
$\nu_{48}+\nu_{12}+\nu_{13}+\nu_{16}$	2638.1	−2.8	0.3	
$\nu_{45}+\nu_6$	2668.4	−4.9	0.8	7
$\nu_{39}+\nu_{12}$	2701.3	−1.7	0.5	7
$\nu_{38}+\nu_{12}$	2736.8	−3.7	0.9	
$\nu_{44}+\nu_6$,	2762.5	−3.2	0.5	
and/or $\nu_{48}+\nu_{14}+\nu_6$		−0.2		
$\nu_{48}+2\nu_{12}+\nu_{16}$	2784.8	−1.3	0.7	
$\nu_{48}+3\nu_{16}+\nu_6$	2803.3	−1.7	0.2	
$\nu_{48}+\nu_{16}+\nu_{12}+\nu_{11}$	2834.6	−1.8	0.4	
$\nu_{48}+\nu_{13}+\nu_6$	2875.0	−2.9	0.5	
$\nu_{45}+\nu_6+\nu_{16}$	3002.6	−4.3	0.5	
$\nu_{48}+\nu_{12}+\nu_6$	3020.3	−2.8	1.9	
$\nu_{39}+\nu_{12}+\nu_{16}$	3036.0	−2.7	0.2	
$\nu_{38}+\nu_{12}+\nu_{16}$	3073.5	−0.4	0.8	
$\nu_{48}+\nu_{16}+\nu_{13}+\nu_6$	3208.9	−4.7		
$\nu_{38}+\nu_6$	3267.3	−8.4	0.7	
$\nu_{38}+\nu_6$	3303.3	−9.6	1.0	
$\nu_{48}+\nu_{12}+\nu_6+\nu_{16}$	3353.8	−5.0	0.7	
$\nu_{48}+2\nu_6$	3577.6	−18.2	1.1	
$\nu_{48}+2\nu_6$	3586.1	−9.7	0.9	
$\nu_{39}+\nu_6+\nu_{16}$	3599.4	−12.0	0.3	
$\nu_{38}+\nu_6+\nu_{16}$	3635.6	−13.0	0.4	
$\nu_{48}+\nu_{12}+\nu_6+2\nu_{16}$	3688.0	−6.5	0.1	
$\nu_{48}+2\nu_6+\nu_{16}$	3910.4	−21.1	0.6	
$\nu_{48}+2\nu_6+\nu_{16}$	3919.9	−11.6	0.3	
$\nu_{48}+2\nu_6+2\nu_{16}$,	4243.4	−23.8	0.2	
and/or $\nu_{48}+\nu_6+2\nu_{12}$		−4.9		

[a]The vibrational numbering of Ref. 37 is used throughout the text.
[b]Two-photon spectra were not normalized for laser power, hence the relative intensities are not given.
[c]"*Cis,trans*" indicates the bands which are thought to be due to the *cis,trans*-octatetraene impurity.
[d]Assignments in parentheses should be considered as tentative.

simplest and the most compelling justification for the assignment of the carrier to *trans,trans*-octatetraene. The origin in the two-photon excitation spectrum is 76.2 cm^{-1} lower in energy than the origin of the one-photon spectrum, the difference corresponding to one quantum of the lowest energy b_u mode ν_{48} ("O_{48}"). Identical shifts are seen for many other bands. These correspond to a_g modes which appear in combination with ν_{48} in the one-photon spectrum. The bands in the one-photon spectrum which do not have a counterpart in the two-photon spectrum are higher frequency b_u promoting modes such as ν_{47} and ν_{46} and their combination bands with a_g modes. The complete

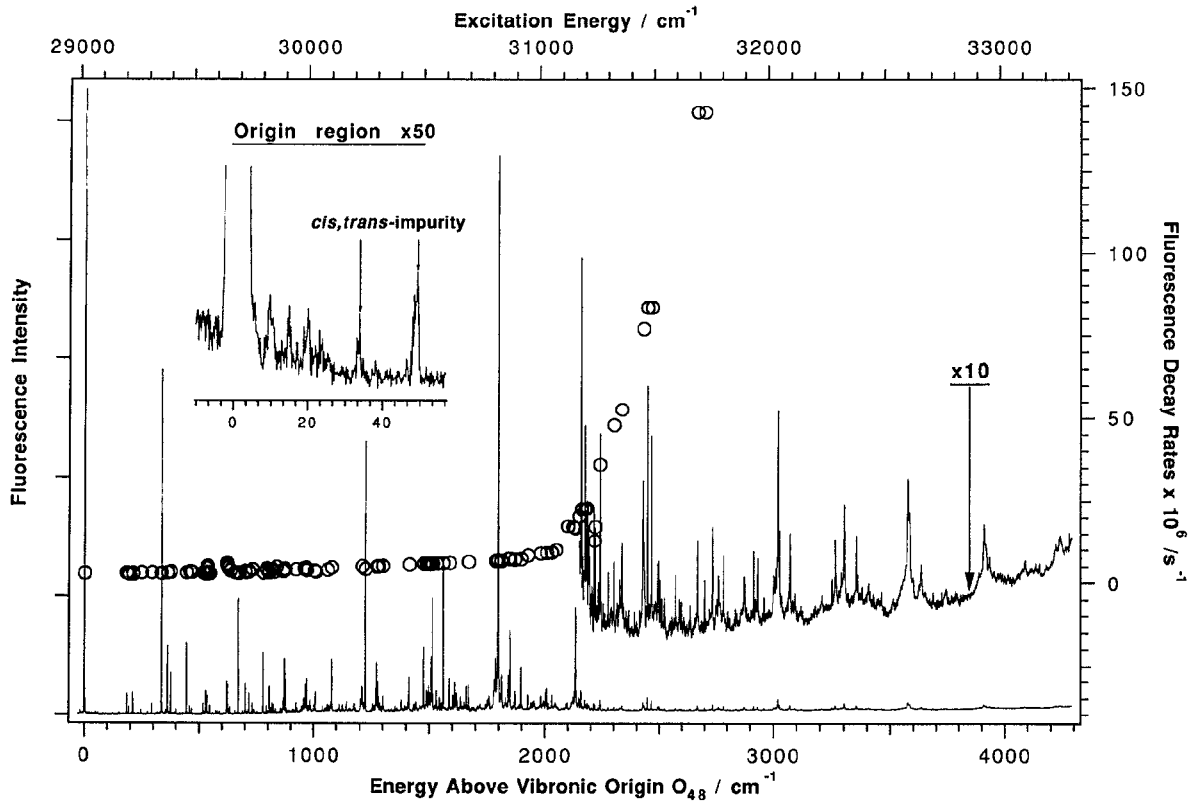

FIG. 3. The one-photon fluorescence excitation spectrum of the 2 $^1A_g \leftarrow 1\ ^1A_g$ transition of *all-trans*-1,3,5,7-octatetraene in a He free jet expansion. The upper axis gives the excitation frequency and the lower axis the energy above the first b_u symmetry $1 \leftarrow 0$ origin at 29 024.9 cm^{-1} (O_{48}). The insert of the origin region is expanded vertically to show the lines due to the *cis,trans*-octatetraene impurity. The open circles give the fluorescence decay rates, which have been measured for some of the stronger transitions.

lack of overlap between vibronic bands in the two spectra proves that the one-photon ($g \rightarrow u$) and two-photon ($g \rightarrow g$) selection rules are strictly obeyed, excluding *cis,trans*-octatetraene as the carrier of the spectrum. The *cis,cis* isomer cannot be excluded on grounds of symmetry, but it is significantly less stable than the other two isomers and none of the spectroscopic information suggests that it could be present. The energies, relative intensities, and lifetimes of the one- and two-photon spectra are presented in Table I. A more detailed analysis of the two-photon spectra of *trans,trans*-octatetraene will be presented in the future.

Further support for assigning *trans,trans*-octatetraene as the carrier comes from a variety of more conventional spectroscopic evidence: (i) comparison of $S_2 \leftarrow S_0$ absorption and fluorescence excitation spectra in Fig. 1; (ii) vibronic analysis of the one-photon $S_1 \leftarrow S_0$ excitation spectrum, including the detailed investigation of hot-band structure; (iii) analysis of $S_1 \rightarrow S_0$ emission spectra; and (iv) S_1 fluorescence lifetime measurements. Given the clear comparison of the one- and two-photon excitation spectra, recitation of additional arguments may seem redundant. However, it is important to demonstrate that an unambiguous assignment of the carrier can be established even without reference to the two-photon spectrum. This will be crucial issue for studies of other polyenes for which the two-photon $S_1 \leftarrow S_0$ spectrum may be difficult to obtain.

B. Analysis of the one-photon 2 $^1A_g \leftarrow 1\ ^1A_g$ spectrum of *trans,trans*-octatetraene

Figure 3 gives the one-photon fluorescence excitation spectrum of the 2 $^1A_g \leftarrow 1\ ^1A_g$ transition of *trans,trans*-1,3,5,7-octatetraene in a He free jet expansion along with fluorescence decay rates of the stronger vibronic bands. A higher resolution spectrum covering the region 0–1000 cm^{-1} above the origin at 29 024.9 cm^{-1} is presented in Fig. 4, along with the fluorescence lifetimes. The assignment of the one-photon spectra in Figs. 3 and 4 to the symmetry forbidden 2 $^1A_g \leftarrow 1\ ^1A_g$ transition of *trans,trans*-1,3,5,7-octatetraene is supported by (i) analysis of the hot-band vibronic structure; (ii) presence of intense $1 \leftarrow 0$ origins of b_u vibronic symmetry; and (iii) progressions in a_g symmetry overtones and combination bands built on b_u $1 \leftarrow 0$ origins. In analyzing the spectra, we have been guided by the one- and two-photon 2 $^1A_g \leftarrow 1\ ^1A_g$ fluorescence excitation and emission spectra of *trans,trans*-octatetraene in an *n*-octane host crystal at 4.2 K (under these conditions, the inversion symmetry of octatetraene is rigorously maintained),[24] room temperature infrared and Raman spectra

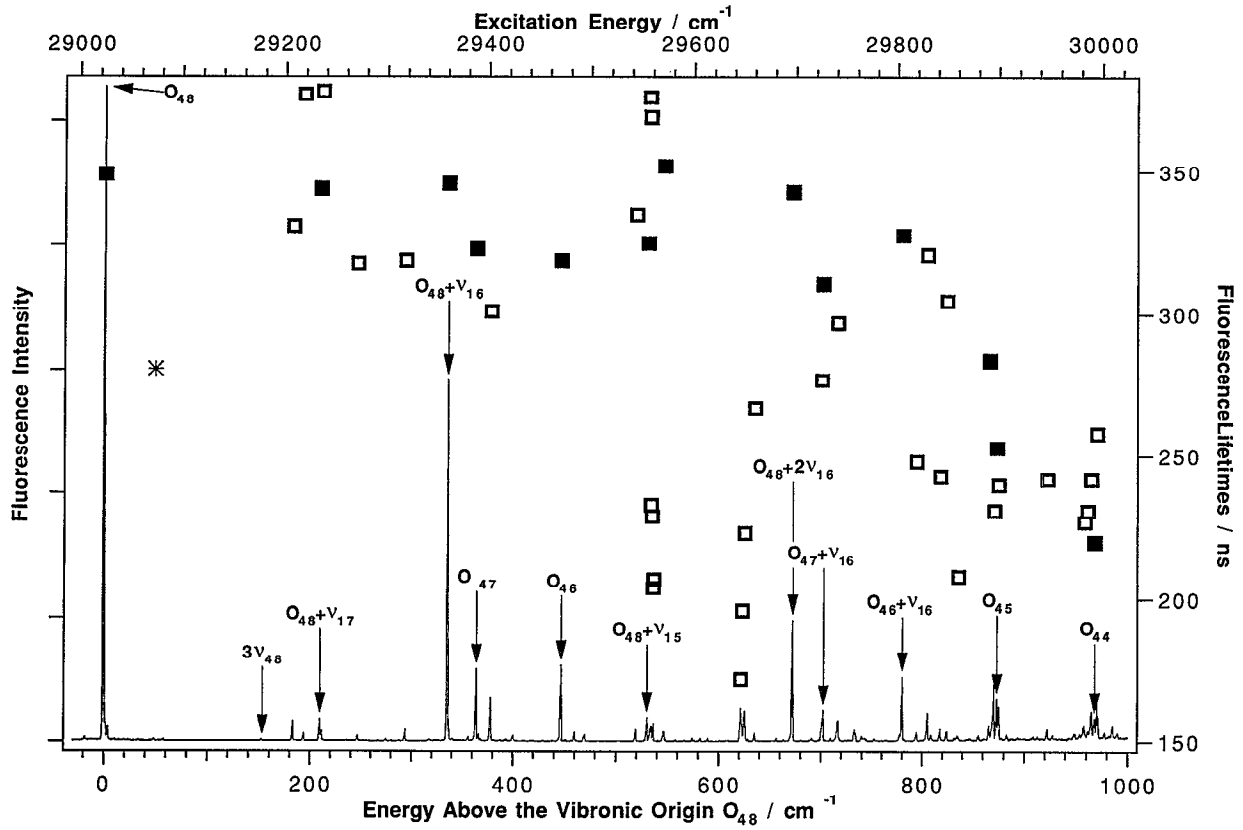

FIG. 4. An expanded portion of the spectrum in Fig. 3 showing the vibrational assignments and fluorescence lifetimes in the 0–1000 cm^{-1} spectral region above O_{48}, the $1\leftarrow0$ origin due to the excitation of one quantum in the b_u symmetry ν_{48} mode. Other b_u $1\leftarrow0$ origins are indicated in the same manner. Full squares represent the lifetimes for the assigned lines, open squares are for the unassigned ones, and the asterisk is for the *cis,trans*-octatetraene impurity. The lifetimes of assigned lines decrease with energy from 341 ns at the origin in a relatively monotonic manner, while the lifetimes of unassigned lines have considerably larger deviations from the average.

of the S_0 state,[37] and theoretical calculations.[26,27] The S_1 and S_0 vibrational frequencies determined in this work are presented in Tables II and III together with previous condensed phase and theoretical frequencies which are the basis for assignments.

1. Assignment of the electronic origin of the 2 $^1A_g\leftarrow1$ ^1A_g spectrum from the hot-band structure

In this section, we use the hot-band structure of the one-photon spectrum to find the electronic origin of the 2 $^1A_g\leftarrow1$ ^1A_g transition and to show that the origin of the one-photon spectrum in Figs. 2–4 is a $1\leftarrow0$ transition in the lowest energy in-plane-bending b_u vibration. The one-photon, vibronic origin at 29 024.9 cm^{-1} will be referred to as O_{48}. The condensed phase frequencies of ν_{48} are 96 and 93 cm^{-1} in the S_0 and S_1 states.[24,37] If ν'_{48} had the same frequency in the gas phase as in *n*-octane,[24] the electronic origin $(0\leftarrow0)$ would be expected at $\sim$28 932 cm^{-1}. In a one-photon vibronically allowed 2 $^1A_g\leftarrow1$ ^1A_g transition, the electronic origin of 2 ^1A_g only can be accessed by $\Delta v=-1$ excitation from b_u vibronic states of 1 ^1A_g. Since ν''_{48} also is the lowest energy b_u promoting mode, spectra of vibrationally warm octatetraene should show prominent $\Delta v=\pm1$ transitions from states with one or more quanta in ν''_{48}:$\Delta v=+1$ transitions will form a sequence starting with O_{48}, while $\Delta v=-1$ transitions will form another sequence starting from $0'\leftarrow1''$ at an energy corresponding to $\nu''_{48}+\nu'_{48}$ below the O_{48}. Condensed phase frequencies for ν''_{48} and ν'_{48} place this transition at $\sim$28 836 cm^{-1}. Figure 5 shows spectra of the one-photon spectrum origin region corresponding to three different vibrational temperatures. Two sequences appear with the $\Delta v=+1$ bands starting from O_{48} and the $\Delta v=-1$ bands starting from 28 862.0 cm^{-1}. The discrepancy between the predicted and observed origins of the $\Delta v=-1$ sequence can be rationalized by the solvent dependence of ν_{48} frequencies in the ground and excited states. From the observed sequence bands, we can calculate the energy of the electronic origin, the frequencies of ν'_{48} and ν''_{48} and estimate their anharmonicities.

The relative intensities and the extent of vibrational cooling at higher He stagnation pressures provide the basis for assigning the sequence bands as shown in Fig. 5. The $\sim$10 cm^{-1} shift to lower energy of successive members of each progression is due to a $\sim$10 cm^{-1} decrease of the ν_{48} frequency in the S_1 state from its S_0 value. The shadings of rotational line shapes to high energy for $\Delta v=-1$ transitions and to low energy for the $\Delta v=+1$ transitions probably are due to differences in rotational constants induced

TABLE II. A comparison of frequencies of fundamental vibrations in the S_1 state determined for *trans,trans*-octatetraene and *cis,trans*-octatetraene in free jet expansions and mixed crystals. The *cis,trans*-octatetraene vibrational frequencies measured in mixed crystals are given next to *trans,trans* frequencies with the closest resemblance. All frequencies are in units of cm^{-1}.

Assignment	*Trans,trans* supersonic jet[a]	*Trans,trans*[c] supersonic jet[a]	*Trans,trans*[d] mixed crystal	*Cis, trans*[e] mixed crystal	*All-trans* theory[f]
a_g					
ν_{17}	209.7	210	219	213	259
ν_{16}	335.7	336	341	393	334
ν_{15}	529.9	538	530	497	604
ν_{14}	964.8				958
ν_{13}	1080.0	1080			1137
ν_{12}	1225.2	1226	1221	1128, 1226	1220
ν_{11}	1275.5	1275	1271	1320	1267
ν_{10}	(1279.6)[b]				1323
ν_9	(1283.8)				1350
ν_8					1464
ν_7	1508.7	1509		1508	1487
ν_6	1797.9	1799	1754	1722	1711
ν_5					2982
ν_4					3063
ν_3					3077
ν_2					3083
ν_1					3095
b_u					
ν_{48}	76.2	76.2	93		106
ν_{47}	439.9	440	463		435
ν_{46}	522.9	524	538		590
ν_{45}	951.6				940
ν_{44}	1044.0	1044	1054		1054
ν_{43}					1195
ν_{42}					1240
ν_{41}					1320
ν_{40}					1357
ν_{39}	1554.0	1555			1463
ν_{38}	1591.2	1592			1543
ν_{37}					2981
ν_{36}					3063
ν_{35}					3079
ν_{34}					3089
ν_{33}					3099

[a]The frequency for ν_{48} of 76.2 cm^{-1} from this work has been used to calculate frequencies of all other b_u symmetry $1\leftarrow 0$ fundamentals measured in the gas phase.
[b]Assignments in parentheses should be considered as tentative.
[c]Reference 35.
[d]Reference 24.
[e]Reference 29.
[f]Reference 27.

by in-plane bending in the lower and upper states of the transitions. The energy ordering of the initial states within a sequence was deduced by observing the effect of vibrational cooling at higher He stagnation pressures. Even at the lowest He stagnation pressure, most of the octatetraene is vibrationally cold, with only a small fraction of molecules populating the low frequency bending and torsional modes. Although there are a number of S_0 vibronic states with <300 cm^{-1} energy, only ν''_{48} appears with significant intensity because it is both the lowest frequency and the strongest b_u promoting mode.

We assume that the energies of ν_{48} vibronic states are given by the anharmonic oscillator expression

TABLE III. The measured S_0 state vibrational frequencies from the emission spectra of isolated *trans,trans*-octatetraene and a comparison with either previously observed solution phase measurements, where available, or theoretically calculated values. All measurements are in units of cm^{-1}.

Assignment	Frequency	Reference 37
a_g		
ν_6	1622	1613
ν_{12}	1179	1179
ν_{16}	340	343
ν_{17}	220	219[a]
b_u		
ν_{46}	577	565
ν_{47}	384	390
ν_{48}	86.5	96

[a]Calculated frequency.

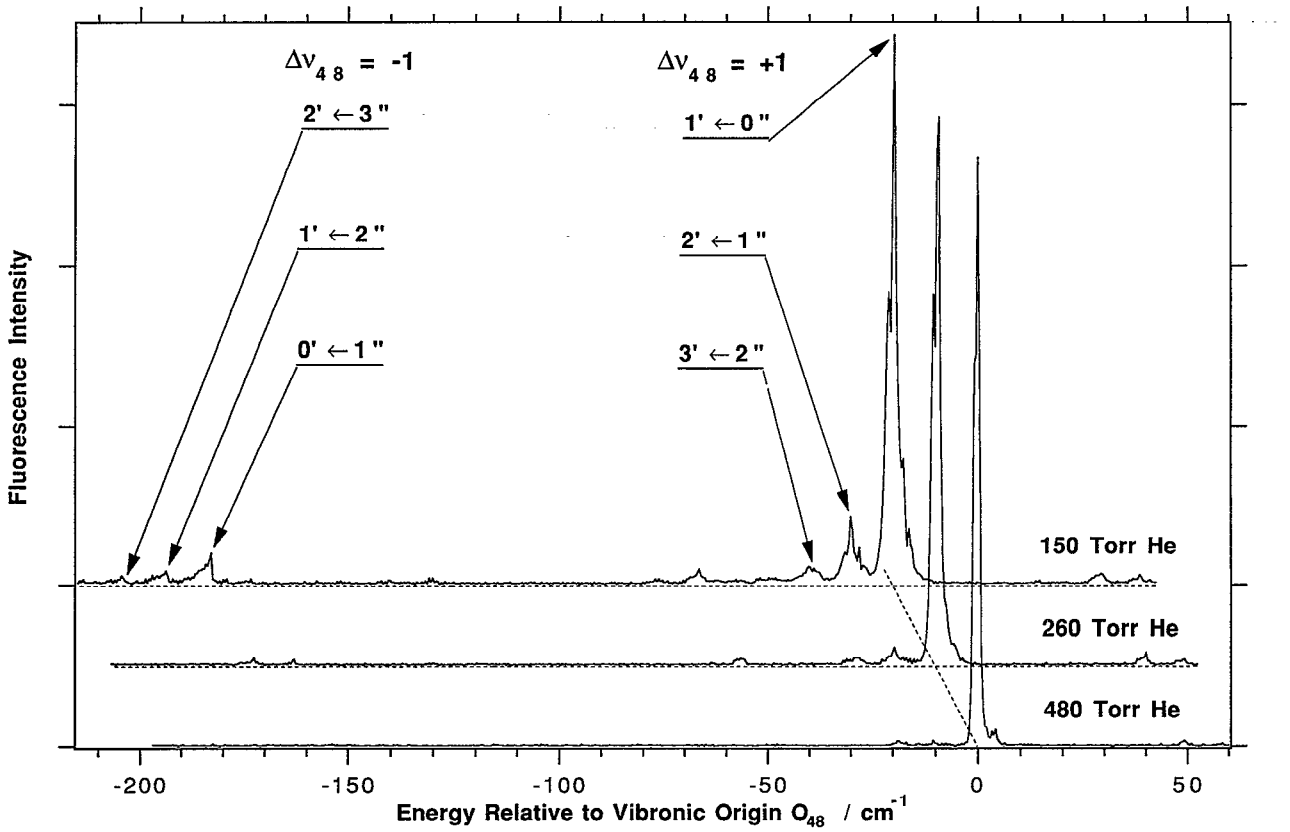

FIG. 5. Fluorescence excitation spectra of the origin region taken at He stagnation pressures of 150, 260, and 480 Torr. The spectra show the vibronic origin of the spectrum O_{48}, as well as several hot-band transitions at lower frequencies. For higher He stagnation pressures, hot-band transitions decrease in intensity due to vibrational cooling. The two sequences of bands correspond to $\Delta v=-1$ and $\Delta v=+1$ transitions in the ν_{48} promoting mode.

$$G_v=T_0+\omega_e(v+\tfrac{1}{2})-\omega_e x_e(v+\tfrac{1}{2})^2, \tag{1}$$

where T_0 contains the contributions to zero-point energy of all modes except for the ν_{48}. The frequency of O_{48} is given by

$$E_{1'-0''}=T_0+\tfrac{3}{2}\omega_e'-(\tfrac{3}{2})^2\,\omega_e x_e'-\tfrac{1}{2}\omega_e''+(\tfrac{1}{2})^2\,\omega_e x_e'', \tag{2}$$

and that of the first (most intense) $\Delta v=-1$ hot band by

$$E_{0'-1''}=T_0+\tfrac{1}{2}\omega_e'-(\tfrac{1}{2})^2\,\omega_e x_e'-\tfrac{3}{2}\omega_e''+(\tfrac{3}{2})^2\,\omega_e x_e''. \tag{3}$$

Using the appropriate relations for the frequencies of other bands, we can derive the following expressions:

$$\Delta_{2''-0''}=E_{1'-0''}-E_{1'-2''}=2\omega_e''-12\omega_e x_e''=173.7\ \text{cm}^{-1}, \tag{4}$$

$$\Delta_{2'-0'}=E_{2'-1''}-E_{0'-1''}=2\omega_e'-12\omega_e x_e'=152.8\ \text{cm}^{-1}, \tag{5}$$

$$\Delta_{3''-1''}=E_{2'-3''}-E_{2'-1''}=2\omega_e''-20\omega_e x_e''=174.4\ \text{cm}^{-1}, \tag{6}$$

$$\Delta_{3'-1'}=E_{3'-2''}-E_{1'-2''}=2\omega_e'-20\omega_e x_e'=153.5\ \text{cm}^{-1}. \tag{7}$$

Equations (4)–(7) allow the determination of the harmonic frequencies and anharmonicities for ν_{48} in the ground and excited states, and these can be used to calculate frequency of the $2\,^1A_g\leftarrow 1\,^1A_g$ electronic origin (Table IV). The ν_{48}' frequency is exactly the same as the energy difference between the one- and two-photon origins. That the excited state frequency is significantly lower than the ground state frequency and both of the anharmonicities are negative may be due to vibronic coupling between the S_1 and S_2 states.[38,39] Another manifestation of vibronic coupling is that the relative intensity of $\Delta v=+1$ transitions is

TABLE IV. The molecular parameters derived in the analysis of the hot-band structure and their comparison with mixed crystal results. All parameters are in units of cm^{-1}.

Parameter	Molecular beam	Condensed phase
0–0	28 948.7[a]	28 561[b]
O_{48}	29 024.9	28 654[b]
ω_e'	75.9	⋯
ω_e''	86.3	⋯
$\omega_e x_e'$	0.089	⋯
$\omega_e x_e''$	0.090	⋯
ν_{48}'	76.2	93[b]
ν_{48}''	86.7	96[c]

[a]The analysis of hot-band structure and the two-photon spectroscopy give the same energy for the electronic origin of the $S_1\leftarrow S_0$ spectrum.
[b]Reference 24.
[c]Reference 37.

about twice as large as that in $\Delta v=-1$ transitions. This propensity is also seen in the emission spectra.

The assignment of the vibrational hot-band structure to sequence bands in the ν_{48} mode can be verified by other features in the fluorescence excitation and emission spectra. Although $\Delta v>|1|$ transitions are expected to be very weak for antisymmetric vibrations, it is possible to detect a weak band 153.1 cm^{-1} above O_{48}, which may be due to the $3'\leftarrow 0''$ transition in the ν_{48} mode. The difference between $3'\leftarrow 0''$ and O_{48} gives an independent measure of $\Delta_{3'-1'}$ from Eq. (7). Further confirmation is provided by emission spectra where $\Delta_{2''-0''}$ of 173 cm^{-1} appears in spectra from modes containing one quantum of ν'_{48} (see below).

The hot-band structure and low frequency lines in the fluorescence excitation and emission spectra are only consistent with the symmetry forbidden $2\,^1A_g\leftarrow 1\,^1A_g$ transition of *trans,trans*-octatetraene. If the spectra were due to the *cis,trans* isomer, then the lowest frequency $0'\leftarrow 1''$ transitions would be shifted from the allowed electronic origin ($0'\leftarrow 0''$) by an amount given by the frequencies of the lowest frequency modes in the condensed phase emission spectra of the *cis,trans* isomer. These are at 29, 51, 120, and 345 cm^{-1}.[29] None of the observed hot bands correspond to these ground state frequencies. Likewise, the emission spectra (see below) show no evidence for these frequencies except for a 345 cm^{-1} mode which is present in both isomers.[24,29] In the region of $\Delta v=-1$ transitions, we observe three bands at ~ -162, -173, and -184 cm^{-1}. These must be assigned as sequence bands, since neither isomer is expected to have three vibrations with such closely spaced frequencies. These bands cannot be assigned to the *cis,trans* isomer because (i) there is no known ground state fundamental at 162 cm^{-1}; (ii) population of several quanta in the 162 cm^{-1} mode would imply a high vibrational temperature and other hot bands then should be observed; (iii) if the 162 cm^{-1} mode appears in hot-band absorption, it also should be observed in emission, and it is not. The assignment of the sequence bands to vibrational excitation in the ν_{48} mode of *trans,trans*-octatetraene requires a much lower vibrational temperature and is also consistent with frequencies measured in emission spectra (see below) and the fluorescence excitation spectrum of the cold molecule. The intensity distribution of the hot bands may not be of a statistical ensemble with a well-defined vibrational temperature. However, there is no *a priori* reason for statistical (Boltzmann) energy distributions in free jet expansions, and since the ν_{48} mode strongly couples both the S_1 and S_0 states with the S_2 state, the transition moment should depend on the displacement along this coordinate.

2. b_u promoting modes

In condensed phase spectra of *trans,trans*-octatetraene, other b_u modes also appear as $1\leftarrow 0$ origins. Vibronic origins due to b_u modes [ν'_{48} (93 cm^{-1}), ν'_{47} (463 cm^{-1}), ν'_{46} (538 cm^{-1}), and ν'_{44} (1054 cm^{-1})] share the following characteristics: (i) they are relatively strong; (ii) they cannot be assigned as overtones or combination bands of lower frequency vibrations; (iii) they do not appear as even overtones or in combination with other b_u modes, or as fundamentals in two-photon spectra; and (iv) they are origins for progressions in a_g modes with a common intensity pattern, which is also seen for the two-photon spectrum.

In the jet, the corresponding b_u modes have frequencies of 76.2 (ν'_{48}), 439.9 (ν'_{47}), 522.9 (ν'_{46}), and 1044.0 (ν'_{44}) cm^{-1}. Comparison of frequencies for isolated molecules and those in mixed crystals in Table II shows a systematic decrease in the gas phase.[24] In the CC stretching region, ν'_{38} and ν'_{39} also have relatively strong intensities. This is consistent with calculations of S_2–S_1 coupling matrix elements, which are relatively large for these b_u modes.[40] However, these are not major features in mixed crystal spectra.

3. Franck–Condon active a_g modes

Other intense bands in the one-photon excitation spectra of *trans,trans*-octatetraene in mixed crystals involve totally symmetric modes which build on b_u $1\leftarrow 0$ origins. The prominent a_g modes of *trans,trans*-octatetraene in *n*-octane at 4.2 K are at 219 (ν'_{17}), 340 (ν'_{16}), 530 (ν'_{15}), 1221 (ν'_{12}), 1271 (ν'_{11}), and 1754 cm^{-1} (ν'_6) (see Table II).[24] Corresponding bands with frequencies of 209.7, 335.7, 529.9, 1225.2, 1275.5, and 1797.9 cm^{-1} are found in the spectrum in Fig. 3. In Table II, comparison of isolated molecule frequencies with condensed phase results for *trans,trans*- and *cis,trans*-octatetraene shows that the agreement is much better for the *trans,trans* isomer. To assign the spectrum to *cis,trans*-octatetraene, it would be necessary to invoke large solvent shifts as was done in the 2C-RE2PI study.[35] If the spectrum is assigned to the *trans,trans* isomer, only ν'_6 has a significant solvent shift ($+28$ and $+44$ cm^{-1} compared to *n*-hexane and *n*-octane, respectively).[24] Since this mode plays an important part in coupling of ^1A_g electronic states, its frequency may be very sensitive to changes in electronic structure upon solvation.[26,27]

The vibrational development seen in Figs. 3 and 4 is dominated by combinations and overtones of the most intense a_g modes (ν'_6, ν'_{12}, and ν'_{16}), which are built on prominent b_u Herzberg–Teller promoting modes (O_{48}, O_{47}; and O_{46}, O_{39}, and O_{38}). The Franck–Condon activity of these totally symmetric modes is attributed to bond order inversion between the S_0 and S_1 states,[1–3,26,27] which results in relatively large displacements for these three modes.[26,40] A progression in ν'_{16} can be observed up to the third overtone and in combination with other a_g modes up to the second overtone. The contributions of ν'_{12} and ν'_6 to the Franck–Condon development are not so obvious in the fluorescence excitation spectrum due to the limited scan range and the increase in nonradiative decay rates at high excess energies. However, these two modes dominate the emission spectra (see below). The absorption intensity maximum of the $S_1\leftarrow S_0$ spectrum probably occurs for $\Delta v>0$ in ν_6 as for methyl substituted tetraenes.[19] The intensity of the ν'_6 fundamental band in the fluorescence excitation spectrum most likely is reduced by faster nonradiative decay at higher excess energies. Other a_g modes such as ν'_{17} at 209.7 cm^{-1} and ν'_{15} at 529.9 cm^{-1} also are present, but have considerably smaller Franck–Condon factors than modes

involving CC stretches. In contrast to the S_1 state, the ν'_{17} mode is significantly more intense than ν'_{16} in the $S_2 \leftarrow S_0$ fluorescence excitation spectrum (Fig. 1).

4. b_g and a_u modes

The assignments in Table I account for most of the low frequency a_g and b_u vibrational modes. Other low frequency bands, which appear to be due to vibrationally cold *trans,trans*-octatetraene, cannot be assigned to a_g or b_u modes or their combination bands. Emission spectra from these levels terminate in a completely different set of ground state levels, and the lifetimes are significantly different than those of a_g or b_u modes. Since some of these bands appear with essentially the same frequencies and relative intensities in the one- and two-photon spectra, it must be concluded that these are also totally symmetric vibrations of *trans,trans*-octatetraene. Other bands appear only in one-photon spectra, so they either must be due to ungerade bands of *trans,trans*-octatetraene, or to impurities. Their consistent presence in the spectra favors the former assignment. Two possibilities for the assignment of these "extra" bands are considered.

First, the appearance of more a_g and b_u bands than can appear as fundamentals in the C_{2h} molecular symmetry group may be an indication that *trans,trans*-octatetraene has lower symmetry than expected from x-ray crystallography[41] and theoretical calculations.[1,2,26,37,42] Experimental evidence from one- and two-photon spectra proves that the molecule has inversion symmetry, leaving the C_i molecular symmetry group as the only alternative for describing the $S_1 \leftrightarrow S_0$ transition. The b_g and b_u symmetry species in C_{2h}, respectively, correlate with the a_g and a_u of C_i. This will add to the number of gerade and ungerade modes with observable transition moments. Second, it is also possible for nontotally symmetric modes to appear as a_g overtones and combination bands if these states borrow intensity by Fermi resonance (unlikely for so many different bands), or if the potential energy surfaces for S_0 and S_1 states have greatly different curvatures. Calculated vibrational frequencies for the S_1 state are indeed considerably smaller than the ground state frequencies and there is significant Duschinsky rotation for the a_u and b_g modes.[26,43] Extra b_u bands could be due to combination bands of a_u and b_g fundamentals and might gain intensity by quadratic coupling between $2\,^1A_g$ and $1\,^1B_u$ states. Through these mechanisms, overtones and combination bands of several low frequency a_u and b_g modes might have observable intensity, even if C_{2h} symmetry is maintained in the S_0 and S_1 states. Regardless of the mechanism through which these vibrations gain intensity, their presence in the one- and two-photon spectra indicates a more facile distortion from the planar configuration of the S_1 state of *trans,trans*-octatetraene as compared to its ground state. Since a_u and b_g modes include torsional motions of the polyene framework, their appearance in the spectra may help to define the potential surface for *cis–trans* isomerization.

5. Impurity bands

The comparison of one- and two-photon fluorescence spectra and detailed assignments given in previous sections establish that the $2\,^1A_g \leftarrow 1\,^1A_g$ transition of *trans,trans*-octatetraene accounts for most of the bands in the fluorescence excitation spectrum. Significant differences between relative intensities in the fluorescence and 2C-RE2PI spectra are found *only* for bands at 33, 49, 236, and 896 cm^{-1} above the origin. The strongest of these lines at 49 cm^{-1} (see the expanded region in Fig. 3) has $\leqslant 0.3\%$ of the intensity of the spectral origin, as compared to 14% in the 2C-RE2PI spectrum.[35] Quantitative comparisons of intensities measured by the two techniques are difficult to make because both the ionization cross sections and fluorescence quantum yields are not known. However, different techniques are unlikely to produce large discrepancies in the intensities of only four bands. Therefore the bands which appear with significantly higher relative intensity in the 2C-RE2PI spectrum are due most likely to the $\sim 20\%$ *cis,trans*-octatetraene impurity.[35] Furthermore, the 49 cm^{-1} fundamental does not appear in combination with other bands, as assigned in the 2C-RE2PI spectrum. In all cases, these bands can be reassigned in a more consistent fashion to other fundamentals or combination bands of the *trans,trans* isomer.

C. Analysis of $2\,^1A_g \rightarrow 1\,^1A_g$ emission spectra of *trans,trans*-octatetraene

Emission spectra from several low energy vibronic levels of the S_1 state of *trans,trans*-octatetraene are shown in Fig. 6. These spectra show progressions in ν''_{16}, ν''_{12}, and ν''_6 as in the fluorescence excitation spectra. The intensity maxima are shifted 3200–4000 cm^{-1} from the energy of excitation with the most intense transitions being due to combination bands with two quanta of the C=C stretch (ν''_6). Large Stokes shifts of emission maxima characterize the $2\,^1A_g \rightarrow 1\,^1A_g$ spectra of linear polyenes and manifest substantial bond order inversion between the S_1 and S_0 states.[1,2,44] Most of the bands seen in the emission spectra involve the three dominant a_g modes and even quanta of one or more of the antisymmetric b_u promoting modes. Transitions can be seen only for the vibrations which differ by one quantum of a b_u mode. That b_u promoting modes play important roles in emission spectra provides further confirmation for the assignment to the *trans,trans* isomer.

Figures 7 and 8 show details of several spectra that further support the assignments of the fluorescence excitation spectra in Table I. Emission spectra from S_1 vibronic levels involving O_{48} and ν'_{16} are shown in Fig. 6. These spectra are dominated by Franck–Condon active modes ν''_{16}, ν''_{12}, and ν''_6, and show strong emission to states with $\Delta v = \pm 1$ in ν''_{48}. Consequently, $\Delta_{2''-0''}$ [see Eq. (4)] stands out as a prominent feature in the emission. The intensities of $\Delta v = +1$ transitions in ν_{48} are significantly higher than $\Delta v = -1$ transitions. This is best seen in the emission spectrum from $O_{48} + \nu'_{16}$, where the $2\nu''_{48} + n\nu''_{16}$ progression is about twice as strong as the corresponding $n\nu''_{16}$ progression. The enhancement of $\Delta v = +1$ emission in ν_{48} can be attributed to strong vibronic coupling between the S_1 and

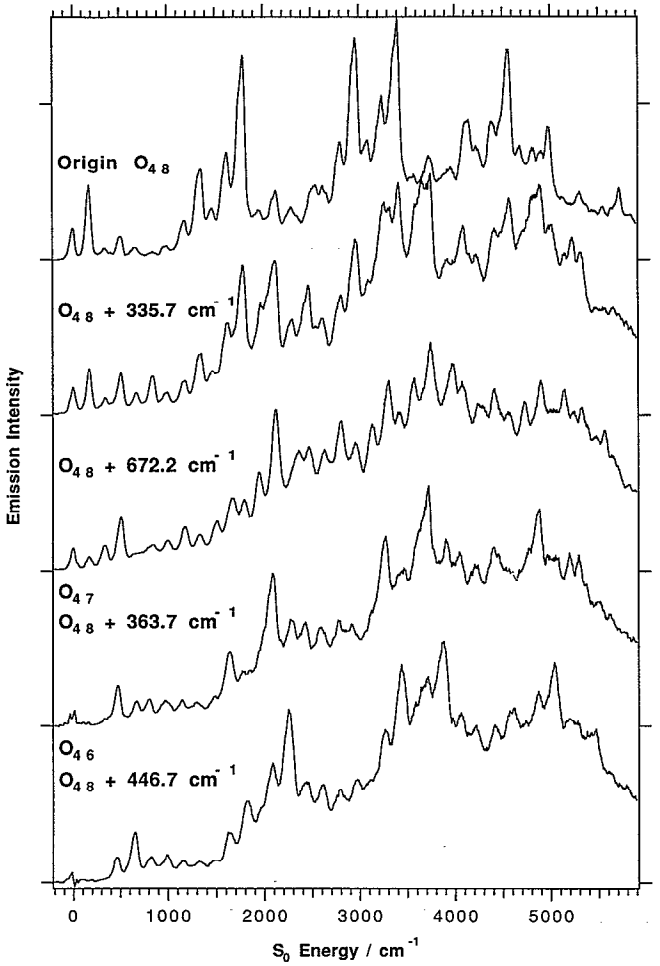

FIG. 6. Representative emission spectra from selected levels in the S_1 state of *trans,trans*-1,3,5,7-octatetraene. The top three spectra originate from O_{48} and the first two members of the progression in the Franck–Condon active ν'_{16} mode. The last two spectra are from b_u promoting modes O_{47} and O_{46}. The emission spectra from the most intense lines can be assigned to progressions in Franck–Condon active ν''_{16}, ν''_{12}, and ν''_6 and $\Delta v = +1$ transitions in the ν_{48} promoting mode.

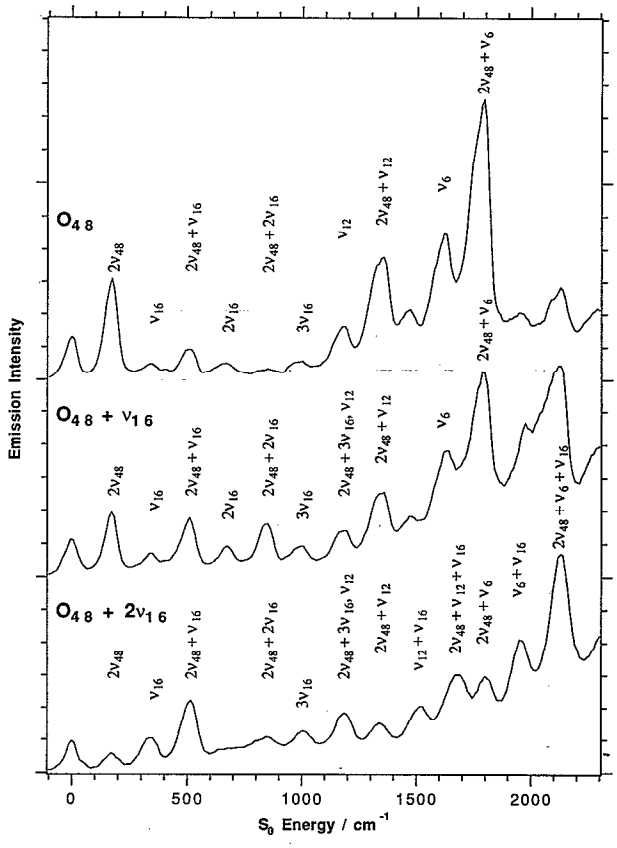

FIG. 7. Expanded emission spectra from O_{48}, $O_{48} + \nu'_{16}$, and $O_{48} + 2\nu'_{16}$ for a Stokes shift of 0–2300 cm^{-1}. The Franck–Condon active ν''_{16} (340 cm^{-1}) contributes to most of the observed structure in these spectra. All of the lines involve $\Delta v = \pm 1$ transitions in the ν_{48} promoting mode.

S_2 states.[38,39] This is also supported by analysis of the Raman activity in the corresponding mode of butadiene in resonance with the S_1 state.[45] Excitation of combination bands of a b_u $1 \leftarrow 0$ origin and an a_g fundamental in most cases results in emission with $\Delta v = +1$ for ν_{48} and $\Delta v = 0$ in all other b_u modes. These intensity patterns of low frequency modes repeat for combination bands with ν''_{12} and ν''_6.

Emission spectra from the three low energy b_u $1 \leftarrow 0$ origins (Fig. 8) also show interesting patterns of vibronic coupling. For emission from O_{48}, the strongest low frequency line is the $\Delta v = +1$ transition to $2\nu''_{48}$ and the rest of the vibrational structure is dominated by a_g combination bands with $2\nu''_{48}$. Since ν_{48} is the strongest promoting mode for the transition, emission spectra from O_{47} and O_{46} are also almost exclusively due to $\Delta v = +1$ transitions in ν_{48}. Other low frequency bands are due to $\Delta v = \pm 1$ in υ_{47} and υ_{46} with a total change of an odd number of quanta in b_u modes. This results in assignment of the vibrational structure in Fig. 8 to binary combinations in b_u modes and their combination bands with ν_{16} ($\Delta v = 0$, 1, or 2). Resonance emissions from O_{47} and O_{46} ($\Delta v = -1$ in ν_{47} and ν_{46}) and first overtones and combination bands ($\Delta\nu_{47} = \Delta\nu_{46} = +1$) are allowed by symmetry, but have very small transition moments compared to $\Delta v = +1$ in ν_{48}. The frequencies of fundamentals that can be unambiguously identified in the emission spectra are given in Table III. The emission spectra are useful for assigning bands with < 1000 cm^{-1} vibrational energy in the S_1 state. At higher energies, fast intramolecular vibrational redistribution (IVR) gives rise to spectral congestion in emission spectra.

D. Fluorescence lifetimes

The fluorescence lifetimes measured in this work (Figs. 3 and 4 and Table I) are considerably different from those reported in the 2C-RE2PI experiments.[35] In comparison with the fluorescence measurements, lifetimes measured by 2C-RE2PI are on the average (i) ~22% shorter for lines below 1080 cm^{-1}; (ii) ~9% longer for lines between 1080.0–1415.7 cm^{-1}; and (iii) ~11% shorter for the higher energy lines. Since the fluorescence method is better suited for lifetime measurements, our lifetimes are more accurate than those from Ref. 35. A possible problem

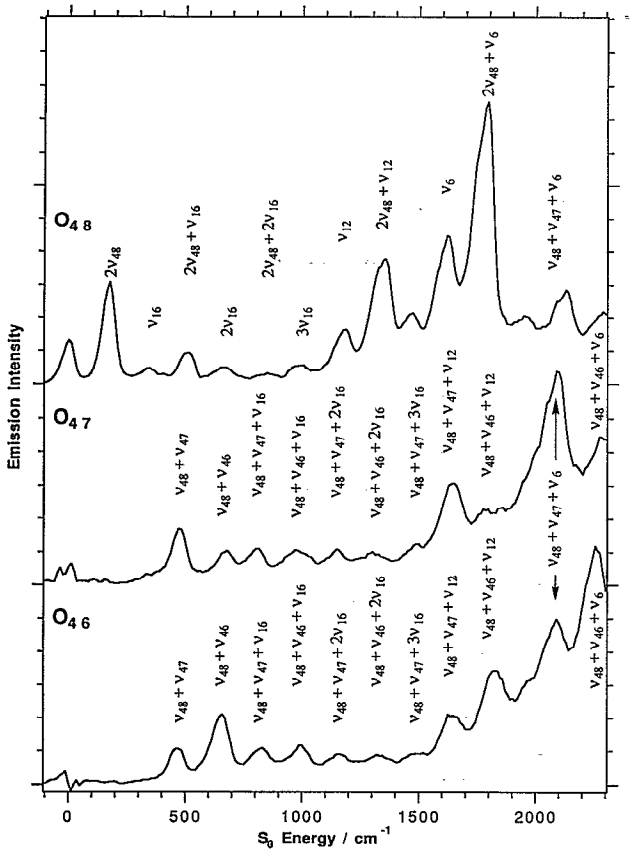

FIG. 8. Expanded emission spectra from the $b_u\,1\leftarrow0$ vibronic origins O_{48}, O_{47}, and O_{46} for a Stokes shift of 0–2300 cm^{-1}. The spectra are dominated by binary combinations of b_u promoting modes and their combination bands with a_g Franck–Condon active modes. In all cases, the most intense lines are due to $\Delta v=+1$ transitions in the ν_{48} promoting mode.

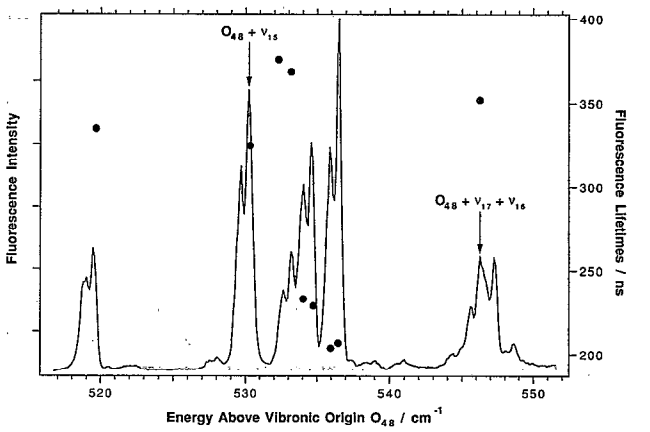

FIG. 9. A detail of the $2\,^1A_g\leftarrow1\,^1A_g$ fluorescence excitation spectrum showing a cluster of lines with nearly the same energy that have significantly different fluorescence lifetimes (indicated by circles). None of the lines with anomalous lifetimes can be assigned to the main progressions in a_g combination bands that start from $b_u\,1\leftarrow0$ origins.

in recording lifetimes by the 2C-RE2PI technique is that molecules can move a considerable distance (~5 mm) during the ~2 μs necessary for the measurements. Accurate measurements of lifetimes by the 2C-RE2PI technique rely on uniformity in the collection efficiency of the ions and the intensity profile of the ionization laser over the interaction volume that the molecules occupy during the measurement. Systematic discrepancies could arise if such conditions are not met.

The fluorescence lifetimes of octatetraene follow the trends previously reported for the methyl-substituted derivatives *trans,trans*-nonatetraene and *trans,trans*-decatetraene.[19,20] The lifetimes near the one-photon origins are ~350 ns for all three tetraenes, which indicates that terminal methyl groups have very little influence on the electronic structure of the tetraene chromophore and do not promote internal conversion to the S_0 state. The fluorescence lifetimes for levels accessed by two-photon excitation are considerably longer (~450 ns) due to the different vibronic coupling mechanisms through which a_g and b_u vibronic states derive optical transition moments. Similar differences in lifetimes for b_u and a_g vibronic states have been observed for one- and two-photon spectra of the $2\,^1A_g\leftarrow1\,^1A_g$ transition of diphenylbutadiene, where at low energies (<600 cm^{-1}), the a_g vibronic symmetry states have $\leqslant2$ times longer lifetimes than the b_u states.[46] It should be emphasized that the octatetraene lifetimes, the longest ever observed for linear polyenes, are consistent with the symmetry-forbidden electronic transitions of centrosymmetric, *all-trans*-polyenes. In fact, the lifetimes are in good agreement with the radiative lifetime of ~220 ns estimated from the fluorescence quantum yield and lifetime of *trans,trans*-octatetraene in room temperature hexane.[32] Radiative lifetimes are expected to be longer in the gas phase than in the solution due to weaker coupling between more widely spaced S_1 and S_2 states.

Octatetraene shows a pronounced quantum state dependence in fluorescence lifetimes 0–1000 cm^{-1} above O_{48}. This can be seen in Figs. 4 and 9, where a high resolution scan shows the lifetimes of several lines in a cluster centered at 535 cm^{-1} above O_{48}. The lifetimes are recorded at P and R branch maxima of selected bands to show the excellent reproducibility of the measurements ($<1\%$ variation for repetitive measurements under the same experimental conditions). The large differences in lifetimes seen in this cluster of lines is typical for this energy region and indicates a pronounced dependence of probably both radiative and nonradiative decay rates on the vibrational state. While the main lines that are assigned to the O_{48}, O_{47}, and O_{46} origins and a_g progressions have lifetimes that decrease monotonically with energy from ~340 ns at O_{48}, there are other unassigned lines (which may be due to a_u or b_g modes; see above) with lifetimes that range between 170 and 380 ns. Corresponding bands in the two-photon spectrum, which are shifted by one quantum of ν'_{48} to lower energy, show parallel trends. Similar quantum state dependent fluorescence decay rates have been observed in nonatetraene and decatetraene, but are much less pronounced.[21] This may be due to a lower density of vibrational states and slower IVR rates in octatetraene.[21]

In the 1000–2100 cm^{-1} energy region, the fluorescence

decay rates increase monotonically. Due to rapid mixing of vibrational modes by IVR, the decay rates most likely are determined by vibronic energy rather than the nature of the excited modes. Similar energy dependent increases in decay rates were observed for nonatetraene and decatetraene and attributed to increases in radiative rates due to energy dependent intensity borrowing from the S_2 state.[19–21] The decrease in lifetimes may also be due to an increase in nonradiative decay rates with increasing energy.[19,20] At $\sim$2100 cm^{-1} above O_{48}, there is a sharp increase in the rate of fluorescence decay. A similar, but less abrupt threshold was observed for the methyl substituted tetraenes.[19,20] The nonradiative decay rate increases more rapidly with excess energy for octatetraene than for methyl substituted derivatives due to a smaller density of vibrational states. The intensity of the fluorescence excitation spectrum drops sharply at this point even though in mixed crystals the absorption strength increases up to the $S_2 \leftarrow S_0$ origin.[24]

The activated nonradiative decay process above the 2100 cm^{-1} barrier may be related to the behavior at lower energies. Below 1000 cm^{-1}, there appears to be little correlation between the intensity of bands and their lifetimes. Therefore, it is unlikely that the differences are merely due to the dependence of radiative decay rates on vibronic states. The putative a_u and b_g torsions with anomalous lifetimes may couple to nonradiative channels more strongly than in-plane modes with b_u or a_g symmetry. The nonradiative decay may be due to enhanced coupling of these modes to the S_0 state,[13] or due to coupling with higher electronic states at large C=C torsional angles, which is believed to occur during *cis–trans* isomerization.[12,15] For higher excitation energies below 2100 cm^{-1}, the decrease in lifetimes may in part be due to tunneling through the barrier for isomerization.

The nonradiative decay of *trans,trans*-octatetraene has also been studied in condensed phases as a function of temperature.[30,31] The temperature dependence of the lifetimes has two regimes, both of which depend on the environment (i) in cyclohexane, the lifetimes drop gradually from 126 to 90 ns between 10 and 179 K; and (ii) at higher temperatures, there is a precipitous drop to 2.5 ns at $\sim$320 K.[30,31] The low temperature process has been ascribed to adiabatic isomerization on the S_1 state surface over a barrier of $\sim$880 cm^{-1} to form electronically excited *cis,trans*-octatetraene.[31,47] A barrier of 1400 cm^{-1} was determined for the high temperature nonradiative decay pathway, but a mechanism has not been proposed.[30,31]

The two temperature regimes for fluorescence decay in the condensed phase may be traced to the same processes that lead to nonradiative decay in isolated octatetraene. The initial drop in the lifetimes at low temperatures in condensed phase may be due to thermal population of the states which are more strongly coupled to nonradiative channels. At higher temperatures, the molecules have sufficient energy to overcome the 1400 cm^{-1} barrier for the activated nonradiative process. However, in gas phase spectra or in lifetime measurements, we find no evidence for adiabatic isomerization to *cis,trans*-octatetraene with an 880 cm^{-1} activation energy on the S_1 surface.

The precipitous drop in the lifetimes at higher energies clearly is due to an activated internal conversion process. A similar phenomenon has been observed for *trans*-stilbene in solution[48] and under isolated conditions.[49] The origin of the barrier for isomerization of *trans*-stilbene is believed to be a crossing between the surfaces of the S_1 and a higher energy ^1A_g electronic state, which occurs at large ethylene torsional angles.[48,49] The barrier height for stilbene changes upon solvation due to differences in the stabilization of the two electronic states by the solvent.[48,49] Since the nonradiative decay of *trans,trans*-octatetraene in condensed and gas phases shows very similar behavior to *trans*-stilbene, we tentatively propose that the nonradiative decay of isolated *trans,trans*-octatetraene above 2100 cm^{-1} excess energy also is due to *trans–cis* isomerization.

E. The relative oscillator strengths of $S_1 \leftrightarrow S_0$ transitions of *cis*- and *trans*-polyenes

The fluorescence excitation spectrum of the $2\,^1A_g \leftarrow 1\,^1A_g$ transition of *trans,trans*-octatetraene (Figs. 3 and 4) is almost identical to the 2C-RE2PI spectrum assigned to the $2\,^1A' \leftarrow 1\,^1A'$ transition of *cis,trans*-octatetraene.[35] The assignment of the 2C-RE2PI spectrum to the *cis,trans* isomer was based, in large part, on the inability of REMPI techniques to detect $S_1 \leftarrow S_0$ spectra of *trans* isomers of hexatriene and alkyl-substituted trienes.[33–35] This was attributed to much weaker transition moments for the symmetry forbidden $2\,^1A_g \leftarrow 1\,^1A_g$ transitions of centrosymmetric, *trans* isomers.[33,34] The results presented in this paper show that both the one- and two-photon $2\,^1A_g \leftarrow 1\,^1A_g$ cross sections of *trans,trans*-octatetraene are sufficiently large to be detected using fluorescence and ionization techniques. In this section, we contrast the fluorescence excitation and 2C-RE2PI spectra and discuss the relative oscillator strengths of *cis*- and *trans*-linear polyenes.

The supposition that the $2\,^1A_g \leftarrow 1\,^1A_g$ transitions of isolated, *all-trans*-polyenes are too weak to observe[35] can be traced to the inability of the REMPI technique to detect the $2\,^1A_g \leftarrow 1\,^1A_g$ spectra of *trans*-trienes. There are two possible explanations for the lack of REMPI signals from *trans*-trienes: (i) the transition moments are considerably weaker for the centrosymmetric *all-trans* isomers; and/or (ii) *trans*-trienes undergo rapid internal conversion to the S_0 state. We recently reported the $S_1 \leftarrow S_0$ fluorescence excitation spectra of *cis*-hexatriene and a *cis* isomer of octatriene from samples that contained mostly *trans* isomers.[28] The spectrum and fluorescence lifetimes indicated that *cis*-hexatriene has at least two separate mechanisms for nonradiative decay—one with no activation energy and another with an activation energy of $<$150 cm^{-1}.[28] The expected origin of the one-photon $2\,^1A_g \leftarrow 1\,^1A_g$ spectrum of *trans*-hexatriene is the $1 \leftarrow 0$ transition in the lowest frequency b_u mode, with a calculated frequency of 174 cm^{-1}.[27] If the activation energy for nonradiative decay were comparable to *cis*-hexatriene, then all of the vibronically allowed transitions of vibrationally cold *trans*-

hexatriene would be above this energy. Assuming that *cis*- and *trans*-hexatriene decay with similar nonradiative decay rates, we would have been unable to detect *trans*-hexatriene fluorescence in our experiment.[28] We conclude that the $2\,^1A_g \leftarrow 1\,^1A_g$ transitions of *all-trans*-trienes have not been observed due to a *combination* of small transition moments and fast nonradiative decays. Finally, it is important to emphasize the danger of making conclusions about the excited state structure and dynamics of tetraenes (the most fluorescent of linear polyenes) based on observations on trienes, considered nonfluorescent until recently.[28]

Comparison of the relative intensities of the origins of $S_1 \leftarrow S_0$ and $S_2 \leftarrow S_0$ fluorescence excitation spectra in mixed crystals for *cis,trans*-(1:20) and *trans,trans*-octatetraene ($1{:}10^5$) suggests that the $S_1 \leftarrow S_0$ spectrum is ~ 5000 stronger for the noncentrosymmetric isomer.[24,29,50] This observation implies that an unattainable level of purity of the *trans,trans* isomer would be necessary to observe the spectrum. Such a comparison of intensities relies on (i) the assumption that the $S_2 \leftarrow S_0$ transition strengths and fluorescence quantum yields are the same for both isomers; (ii) that solutions are optically dilute; and (iii) on correct normalization of fluorescence excitation scans with several laser dyes. Furthermore, the above line of reasoning implies that it would be equally difficult (i.e., impossible) to detect the $2\,^1A_g \leftarrow 1\,^1A_g$ spectrum of any *all-trans*-polyene in a centrosymmetric environment. This clashes with a great number of experiments that have reported fluorescence excitation and emission spectra from *all-trans* linear polyenes in solutions, low temperature glasses, and mixed crystals. Of particular relevance are low temperature, mixed crystal studies in which polyenes exhibit the distinctive pattern of Herzberg–Teller vibronic coupling expected for the symmetry-forbidden $S_1 \leftrightarrow S_0$ transitions of *all-trans* isomers.[1,23,24,31]

Octatetraene fluorescence lifetimes in condensed phases also support the conclusion that $S_1 \leftrightarrow S_0$ transitions in *trans*- and *cis*-tetraenes have comparable oscillator strengths. Lifetimes in 10 K alkane solutions are *trans,trans*- 226 ns (*n*-octane) and 123 ns (*n*-hexane); *cis,cis*- 130 ns (*n*-octane); *cis,trans*- 70 ns (*n*-hexane) and *s-cis*- 29 ns (*n*-octane).[30,51,52] These lifetimes can be compared with the ~ 220 ns *radiative* lifetime of *trans,trans*-octatetraene determined in room temperature hexane.[32] Comparison of the *trans,trans*-S_1 lifetimes in *n*-octane and *n*-hexane[30] is instructive since the $S_1 \leftrightarrow S_0$ spectrum changes from being electronically forbidden to being partially allowed (inversion symmetry is preserved in *n*-octane, but not in *n*-hexane). In spite of the breaking of symmetry, the $S_1 \leftrightarrow S_0$ transition has an oscillator strength at most two times larger for the distorted *trans,trans*-octatetraene (assuming that the fluorescence quantum yield is not greatly influenced by the solvent). Comparison of the S_1 lifetimes of the *cis,cis* ($S_1 \leftrightarrow S_0$ transitions are also symmetry forbidden in *n*-octane), *cis,trans* (symmetry-allowed), and *s-cis* (symmetry-allowed) isomers also indicates relatively small differences in $S_1 \leftrightarrow S_0$ oscillator strengths. For *trans,trans*- and *s-cis*-octatetraene, both the relative fluorescence yields ($\sim 0.36/1$) (Ref. 52) and lifetimes are known. These data imply radiative decay rates for the $2\,^1A_g$ states that are about 20 times smaller for *trans,trans*- than for the *s-cis*-octatetraene. The comparable lifetimes of *trans,trans*- and *cis,trans*-octatetraene suggest an even smaller ratio for the oscillator strengths of their $S_1 \leftrightarrow S_0$ transitions, though the lack of relative fluorescence yields prevents a more quantitative comparison. The measured 281 ns lifetime of the 49 cm^{-1} band in the free jet fluorescence excitation spectra (reassigned to the *cis,trans*-octatetraene in Table I) is useful for comparison of transition strengths under isolated conditions. If the two isomers have equal fluorescence quantum yields, the transition strength for the *cis,trans* isomer is at most twice that of the *trans,trans* isomer. The small differences in fluorescence lifetimes for systems with and without inversion symmetry indicate that the S_1 lifetimes are determined primarily by vibronic coupling with the S_2 state and that this coupling is not very sensitive to the excited state geometries.

V. CONCLUSIONS

Fluorescence excitation and emission spectra of the $S_1 \leftrightarrow S_0$ transitions of *trans,trans*-1,3,5,7-octatetraene have been measured for the first time in free jet expansions. An almost identical spectrum previously had been obtained using the 2C-RE2PI technique and assigned to *cis,trans*-octatetraene.[35] Our assignment of the spectra to the $2\,^1A_g \leftarrow 1\,^1A_g$ transition of *trans,trans*-octatetraene is based on (i) comparison of the one- and two-photon fluorescence excitation spectra; (ii) vibronic analysis of the one-photon $S_1 \leftarrow S_0$ excitation spectrum, including the detailed investigation of hot-band structure and comparison with the vibronic structure previously observed in one- and two-photon fluorescence excitation spectra in the condensed phase; (iii) analysis of $S_1 \rightarrow S_0$ emission spectra from a range of S_1 vibronic levels; (iv) measurement of S_1 fluorescence lifetimes; and (v) the $S_2 \leftarrow S_0$ fluorescence excitation spectrum. The analysis of the spectra provides important structural information on isolated *trans,trans*-octatetraene such as accurate frequencies for a number of a_g and b_u vibrations and the electronic origin of the S_1 state.

The dominance of $\Delta v = +1$ transitions in the lowest frequency b_u in-plane bending vibration (ν_{48}) in the one-photon excitation and emission spectra is consistent with strong Herzberg–Teller coupling between the S_2 and S_1 states. The fluorescence lifetimes of individual S_1 vibronic states depend on the vibronic level excited in the low energy region (< 1000 cm^{-1} excess energy). Anomalous lifetimes are observed for unassigned bands, which may be due to out-of-plane vibrations and torsions of the polyene framework. At ~ 2100 cm^{-1} excess energy, there is a sharp onset of a nonradiative decay process which we tentatively assign to *trans–cis* isomerization.

The discovery of $2\,^1A_g \rightarrow 1\,^1A_g$ emissions in gaseous trienes,[28] tetraenes, and pentaenes[18] now has led to the detection of the $2\,^1A_g \leftarrow 1\,^1A_g$ transitions of several polyenes in supersonic jets using fluorescence excitation techniques.[19,20,28] These experiments have provided the first de-

tailed data on the $2\,^1A_g$ states of isolated, *all-trans* polyenes. Comparison of the one- and two-photon excitation spectra of *trans,trans*-octatetraene under the collision-free conditions offers an unprecedented view of the photophysics of this prototypical molecule. Measurements of the structure and dynamics in the S_2, S_1, and S_0 states of *all-trans*-octatetraene under the collision-free conditions of free-jet expansions provide benchmarks for theoretical calculations and for comparison of the effects of conjugation length, alkyl substitution, and solvent perturbations on the electronic structure of linear polyenes.

ACKNOWLEDGMENTS

We are grateful to M. Tasumi and H. Yoshida for kindly providing advice on the dehydration of 1,4,6-octatriene-3-ol. We thank the Royal Society/Japan Society for the Promotion of Science for support of A.J.B., the Donors of the Petroleum Research Fund, administered by the American Chemical Society, a DuPont Fund grant to Bowdoin College, and the National Science Foundation U.S.–Japan Cooperative Photoconversion and Photosynthesis Research Program (Grant No. INT-9121965) for partial support of research by RLC and BT. We also acknowledge M. Z. Zgierski, S. Saito, D. W. Pratt, I. Ohmine, J. H. Frederick, and M. Aoyagi for invaluable discussions on the electronic structure and dynamics of polyenes, and for providing unpublished results. This work was supported by a grant-in-aid for Scientific Research on New Program (03NP0301) by the Department of Education, Science, and Culture of Japan.

[1] B. S. Hudson, B. E. Kohler, and K. Schulten, in *Excited States*, edited by E. C. Lim (Academic, New York, 1982), Vol. 6, p. 1.
[2] G. Orlandi, F. Zerbetto, and M. Z. Zgierski, Chem. Rev. **91**, 867 (1991).
[3] R. J. Cave and E. R. Davidson, J. Phys. Chem. **92**, 2173 (1988).
[4] T. Yoshizawa and H. Kandori, in *Progress in Retinal Research*, edited by N. N. Osborne and G. J. Chader (Pergamon, Oxford, 1992), Vol. 11, pp. 33–55.
[5] M. Mimuro and T. Katoh, Pure Appl. Chem. **63**, 123 (1991); R. R. Birge, Biochim. Biophys. Acta **1016**, 293 (1990).
[6] S. R. Marder, D. N. Beratan, and L.-T. Cheng, Science **252**, 103 (1991).
[7] B. E. Kohler, *Conjugated Polymers: The Novel Science and Technology of Conducting and Nonlinear Optically Active Materials*, edited by J. L. Bredas and R. Silbey (Kluwer, Dordrecht, 1991), pp. 405–434.
[8] B. S. Hudson and B. E. Kohler, Chem. Phys. Lett. **14**, 299 (1972); J. Chem. Phys. **59**, 4984 (1973).
[9] K. Schulten and M. Karplus, Chem. Phys. Lett. **14**, 305 (1972).
[10] K. Schulten, I. Ohmine, and M. Karplus, J. Chem. Phys. **64**, 4422 (1976); I. Ohmine, K. Schulten, and M. Karplus, *ibid.* **68**, 2348 (1978).
[11] A. P. Shreve, J. K. Trautman, T. G. Owens, and A. C. Albrecht, Chem. Phys. Lett. **178**, 89 (1991).
[12] I. Ohmine, J. Chem. Phys. **83**, 2348 (1985); U. Dinur and B. Scharf, *ibid.* **79**, 2600 (1983).
[13] F. Zerbetto and M. Z. Zgierski, J. Chem. Phys. **93**, 1235 (1990).
[14] V. Bonačić-Koutecky, M. Persico, D. Dohnert, and A. Sevin, J. Am. Chem. Soc. **104**, 6900 (1982).
[15] G. J. M. Dormans, G. C. Groenenboom, and H. M. Buck, J. Chem. Phys. **86**, 4895 (1987).
[16] D. G. Leopold, V. Vaida, and M. F. Granville, J. Chem. Phys. **81**, 4210 (1984); V. Vaida, Acc. Chem. Res. **19**, 114 (1986).
[17] L. A. Heimbrook, J. E. Kenny, B. E. Kohler, and G. W. Scott, J. Chem. Phys. **75**, 4338 (1981).
[18] W. G. Bouwman, A. C. Jones, D. Phillips, P. Thibodeau, C. Friel, and R. L. Christensen, J. Chem. Phys. **94**, 7429 (1990).
[19] H. Petek, A. J. Bell, K. Yoshihara, and R. L. Christensen, J. Chem. Phys. **95**, 4739 (1991).
[20] H. Petek, A. J. Bell, K. Yoshihara, and R. L. Christensen, SPIE Proc. **1638**, 345 (1992); H. Petek, A. J. Bell, H. Kandori, K. Yoshihara, and R. L. Christensen, *Time Resolved Vibrational Spectroscopy*, edited by H. Takahashi (Springer, Berlin, 1992), Vol. 5, pp. 198–199.
[21] H. Petek, A. J. Bell, K. Yoshihara, and R. L. Christensen (to be published).
[22] G. Herzberg and E. Teller, Z. Phys. Chem. B **21**, 410 (1933).
[23] R. L. Christensen and B. E. Kohler, J. Chem. Phys. **63**, 1837 (1975).
[24] M. F. Granville, G. R. Holtom, and B. E. Kohler, J. Chem. Phys. **72**, 4671 (1980); M. F. Granville, G. R. Holtom, B. E. Kohler, R. L. Christensen, and K. L. D'Amico, *ibid.* **70**, 593 (1979).
[25] B. E. Kohler and P. West, J. Chem. Phys. **79**, 583 (1983).
[26] M. Aoyagi, I. Ohmine, and B. E. Kohler, J. Phys. Chem. **94**, 3922 (1990).
[27] F. Zerbetto, M. Z. Zgierski, F. Negri, and G. Orlandi, J. Chem. Phys. **89**, 3681 (1988).
[28] H. Petek, A. J. Bell, K. Yoshihara, and R. L. Christensen, J. Chem. Phys. **96**, 2412 (1992).
[29] B. E. Kohler and T. A. Spiglanin, J. Chem. Phys. **80**, 3091 (1984).
[30] J. R. Ackerman, B. E. Kohler, D. Huppert, and P. M. Rentzepis, J. Chem. Phys. **77**, 3967 (1982).
[31] B. E. Kohler, P. Mitra, and P. West, J. Chem. Phys. **85**, 4436 (1986); J. R. Ackerman and B. E. Kohler, J. Am. Chem. Soc. **106**, 3681 (1984); M. F. Granville, G. R. Holtom, and B. E. Kohler, Proc. Natl. Acad. Sci. USA **77**, 31 (1980).
[32] R. M. Gavin, C. Weisman, J. K. McVey, and S. A. Rice, J. Chem. Phys. **68**, 522 (1978).
[33] W. J. Buma, B. E. Kohler, and K. Song, J. Chem. Phys. **92**, 4622 (1990); **94**, 6367 (1991).
[34] W. J. Buma, B. E. Kohler, and K. Song, J. Chem. Phys. **94**, 4691 (1991).
[35] W. J. Buma, B. E. Kohler, and T. Shaler, J. Chem. Phys. **96**, 399 (1992).
[36] K. L. D'Amico, C. Manos, and R. L. Christensen, J. Am. Chem. Soc. **102**, 1777 (1980).
[37] H. Yoshida and M. Tasumi, J. Chem. Phys. **89**, 2803 (1988); H. Yoshida, Ph. D. thesis, University of Tokyo, 1990.
[38] W. H. Henneker, A. P. Penner, W. Siebrand, and M. Z. Zgierski, J. Chem. Phys. **69**, 1884 (1978); A. R. Gregory, W. H. Henneker, W. Siebrand, and M. Z. Zgierski, *ibid.* **65**, 2071 (1976).
[39] L. Seidner, G. Stock, A. L. Sobolewski, and W. Domcke, J. Chem. Phys. **96**, 5298 (1992).
[40] M. Z. Zgierski (unpublished results).
[41] M. Traetteberg, Acta. Chem. Scand. **22**, 2294 (1968).
[42] M. Aoyagi, Y. Osamura, and S. Iwata, J. Chem. Phys. **83**, 1140 (1985); A. C. Lasaga, R. J. Aerni, and M. Karplus, *ibid.* **73**, 5230 (1980).
[43] F. Duschinsky, Acta Physicochim. URSS **7**, 551 (1937).
[44] S. A. Cosgrove, M. A. Guite, T. B. Burnell, and R. L. Christensen, J. Phys. Chem. **94**, 8118 (1990).
[45] R. R. Chadwick, M. Z. Zgierski, and B. S. Hudson, J. Chem. Phys. **95**, 7204 (1991).
[46] J. S. Horowitz, B. E. Kohler, and T. A. Spiglanin, J. Chem. Phys. **83**, 2186 (1985).
[47] G. Adamson, G. Gradl, and B. E. Kohler, J. Chem. Phys. **90**, 3038 (1989).
[48] D. H. Waldeck, Chem. Rev. **91**, 415 (1991); M. Sumitani, N. Nakashima, K. Yoshihara, and S. Nagakura, Chem. Phys. Lett. **51**, 138 (1977).
[49] J. A. Syage, P. M. Felker, and A. H. Zewail, J. Chem. Phys. **81**, 4706 (1985); J. Troe and J. Schroeder, J. Phys. Chem. **90**, 4215 (1986); A. Amirav and J. Jortner, Chem. Phys. Lett. **95**, 295 (1983).
[50] We thank one of our referees for pointing out this observation.
[51] J. R. Ackerman and B. E. Kohler, J. Chem. Phys. **80**, 45 (1984).
[52] J. R. Ackerman, S. A. Forman, M. Hossain, and B. E. Kohler, J. Chem. Phys. **80**, 39 (1984).